

Large- N reduction in QCD-like theories with massive adjoint fermionsTatsuo Azeayanagi,^{1,*} Masanori Hanada,^{2,†} Mithat Ünsal,^{2,3,‡} and Ran Yacoby^{2,§}¹*Department of Physics, Kyoto University, Kyoto 606-8502, Japan*²*Department of Particle Physics and Astrophysics, Weizmann Institute of Science, Rehovot 76100, Israel*³*SLAC and Physics Department, Stanford University, Stanford, California 94025/94305, USA*

(Received 25 October 2010; published 9 December 2010)

Large- N QCD with heavy adjoint fermions emulates pure Yang-Mills theory at long distances. We study this theory on a four- and three-torus, and analytically argue the existence of a large-small volume equivalence. For any finite mass, the center-symmetry unbroken phase exists at sufficiently small volume and this phase can be used to study the large volume limit through the Eguchi-Kawai equivalence. A finite-temperature version of volume independence implies that thermodynamics on $\mathbb{R}^3 \times S^1$ can be studied via a unitary matrix quantum mechanics on S^1 , by varying the temperature. To confirm this nonperturbatively, we numerically study both zero- and one-dimensional theories by using Monte Carlo simulation. The order of finite- N corrections turns out to be $1/N$. We introduce various twisted versions of the reduced QCD which systematically suppress finite- N corrections. Using a twisted model, we observe the confinement/deconfinement transition on a $1^3 \times 2$ lattice. The result agrees with large volume simulations of Yang-Mills theory. We also comment that the twisted model can serve as a nonperturbative formulation of the noncommutative Yang-Mills theory.

DOI: [10.1103/PhysRevD.82.125013](https://doi.org/10.1103/PhysRevD.82.125013)

PACS numbers: 11.15.Pg, 11.15.Ha

I. INTRODUCTION

Recently Yang-Mills (YM) theory with adjoint fermions, QCD(Adj), has attracted much interest. The main impetus behind this is a network of exact large- N equivalences. The starting point is the large- N orientifold equivalence, which states that the bosonic subsector of this theory is equivalent to the charge-conjugation even subsector of QCD with fermions in antisymmetric representation [QCD(AS)] [1], provided symmetries defining the neutral subsectors are not spontaneously broken [2]. QCD(AS) reduces to the ordinary QCD with fundamental quarks when $N = 3$, and is a natural large- N generalization thereof [3].¹ The second important link is an orbifold equivalence: when quarks are massless or light with respect to strong scale Λ_{QCD} , QCD(Adj) compactified on a Euclidean four-torus exhibits volume independence, thanks to its unbroken prerequisite (center and translational) symmetries at any radius [7]. Thus, through the Eguchi-Kawai (EK) equivalence [8], one can study large- N QCD on \mathbb{R}^4 by using a unitary matrix model on a single-site lattice. QCD(Adj) also provides new insights into gauge dynamics, especially on small $S^1 \times \mathbb{R}^3$. This theory exhibits new nonperturbative phenomena, most strikingly confinement due to magnetic bions, a new class of non-self-dual topological

excitations [9,10], distinct from monopoles and instantons.

The statement of the volume independence [7,8,11,12] is as follows. Consider $SU(N)$ gauge theories on \mathbb{R}^4 , with or without fermions, toroidally compactified on a four manifold $\mathbb{R}^{4-d} \times T^d$. For simplicity, we assume the matter fields are in adjoint representation and, hence, the theory has a global $(\mathbb{Z}_N)^d$ center symmetry, described most easily as gauge rotations aperiodic up to an element of the center group. The order parameters of this symmetry are Wilson lines wrapping distinct toroidal cycles. The observables singlet under the center transformation constitute the neutral sector. The volume independence states that dynamics of the neutral sector observables is independent of the size of the torus provided the center symmetry and translational invariance are not spontaneously broken. Among such observables are nonperturbative mass spectrum, free energy densities, and deconfinement transition temperature, just to count a few. This is clearly an extraordinarily well justified reason to study aspects of the small volume, large- N gauge theories.

In fact, center symmetry is spontaneously broken in most examples. In the original Eguchi-Kawai model [8], which is a one-point reduction of Wilson's bosonic lattice gauge theory, the breakdown can be shown by one-loop calculation around a diagonal background [13]. The quenched [13,14] and twisted [15] modifications of the Eguchi-Kawai model were proposed to preserve the symmetry, but after two decades, it is now understood that both modifications fail nontrivially due to nonperturbative

*aze@gauge.scphys.kyoto-u.ac.jp

†masanori.hanada@weizmann.ac.il

‡unsal@slac.stanford.edu

§ran.yacoby@weizmann.ac.il

¹The phenomenology of QCD(AS) is examined in [4–6].

effects [16–19].² Similarly, in any gauge theory compactified thermally on $\mathbb{R}^3 \times S^1$, or on a torus with at least one thermal boundary condition, center symmetry breaks spontaneously in the high temperature deconfined phase, and volume independence is only valid in the low temperature confined phase, above a critical volume [12].

Kovtun, one of us (M. Ü.), and Yaffe, motivated by the quantitative differences between thermal and circle (non-thermal) compactifications, showed that if light or massless adjoint fermions endowed with periodic boundary conditions are added to Yang-Mills theory, then the center symmetry is stabilized at small volume dynamically [7]. (Also see the discussion in Refs. [24–26].)

For heavy fermions, the infrared physics of QCD(Adj) on \mathbb{R}^4 emulates the bosonic Yang-Mills theory. Since heavy fermions are also capable of restoring center symmetry at sufficiently small volume, this may provide an opportunity for a working Eguchi-Kawai reduction for an “almost” Yang-Mills theory. However, this is not straightforward. When one dimension is compactified, QCD(Adj) with massive fermions on small $S^1 \times \mathbb{R}^3$ exhibits an intricate phase structure. This can be deduced from a one-loop effective action of the Wilson line [25,27], simulations on an asymmetric torus mimicking $S^1 \times \mathbb{R}^3$ [28], and studies on $S^1 \times S^3$ [29] which also mimics $S^1 \times \mathbb{R}^3$ due to topological reasons, as explained in [30]. In all these cases, the \mathbb{Z}_N symmetry along S^1 is intact at large radius, and as one decreases the radius, it breaks down completely at some critical point and then gradually restores to various subgroups of the center symmetry. \mathbb{Z}_N symmetry is restored fully only at $mLN \sim \text{few}$, where L is the compactification radius and m is the fermion mass in continuum. This is troubling because the volume independence (strong coupling, non-Abelian confinement) domain is $LN\Lambda_{\text{YM}} \gg 1$ [31], whereas, for heavy fermions, $m \gtrsim \Lambda_{\text{YM}}$, the first condition implies $LN\Lambda_{\text{YM}} \lesssim \text{few}$ which is a volume dependent, weak-coupling Abelian confinement domain [31].

One might expect a similar pattern for a single-site lattice model based on this weak-coupling intuition. However, recent important work of Bringoltz and Sharpe shows that $(\mathbb{Z}_N)^4$ remains intact in a rather generous “funnel,” in the fermion mass, lattice coupling plane, covering the continuum limit of Yang-Mills theory [32] (also, see [33]), corresponding to the limit where the bare fermion mass is larger than cutoff scale. In particular, they observe a $(\mathbb{Z}_N)^4$ restoration at $ma \sim O(N^0)$, where m is

bare lattice mass and a is lattice spacing. Why and how the full center-symmetry restoration takes place at $ma \sim O(N^0)$ is the main theoretical problem that we wish to address in this work.

Results

To set the notation, we first express the action of continuum QCD(Adj) on a four manifold:

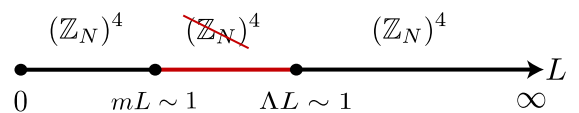
$$S = \frac{N}{\lambda_{4d}} \int_0^\beta dt \int d^3x \text{Tr} \left[\frac{1}{4} F_{\mu\nu}^2 + \sum_{f=1}^{N_f} \bar{\psi}_f (\not{D} + m) \psi_f \right], \quad (1)$$

where ψ_f are Dirac fermions with mass m . (Generalization to different values of masses is straightforward.) In general, we will consider this theory on four-torus $T^3 \times S^1$, with sizes L and β , respectively. If we impose the anti-periodic boundary condition on fermions along the temporal direction, this action describes the finite-temperature system and β corresponds to the inverse temperature. For periodic boundary conditions on fermions in all directions, we consider $\beta = L$, a symmetric four-torus.

We show that, with periodic boundary conditions, $(\mathbb{Z}_N)^4$ symmetry is not broken at sufficiently small- L , although it can be broken at some intermediate volume. [More precisely, $(\mathbb{Z}_N)^4$ symmetric and broken phases can coexist, while quantum tunneling between them is suppressed in the large- N limit.] The argument, which will be quantified in Sec. III A, is very simple—although the one-loop effective action suggests the existence of the attraction between Wilson line eigenvalues at small separation, the eigenvalues spread due to nonperturbative quantum fluctuations [34], and the one-loop calculation can be trusted only at large separations where it leads to repulsion. The estimates of nonperturbative fluctuations are outside the reach of one-loop perturbation theory and often overwhelm the implications of one-loop analysis. Because of nonperturbative effects, we find that the full center restoration takes place at $mL \sim O(N^0)$, which is compatible with $LN\Lambda_{\text{YM}} \gg 1$ for $m \gtrsim \Lambda_{\text{YM}}$.

Our main results are

- (1) *Small-large volume equivalence:* The QCD(Adj) with heavy fermions of mass m on \mathbb{R}^4 , or T^4 with radii $L \gtrsim \Lambda^{-1}$, is equivalent to the theory on a small T^4 , with radii $mL < O(N^0)$, due to unbroken $(\mathbb{Z}_N)^4$ center symmetry associated with the cycles on T^4 . This is a small-large volume equivalence with an intermediate center-symmetry broken phase, where volume independence is not valid. This is depicted in the following figure.



- (2) *Finite-temperature equivalence:* The theory on $\mathbb{R}^3 \times S^1$ at finite temperature is equivalent to the

²The failure of these modifications can be cured by introducing supersymmetry [19,20]. Reference [21] proposed a concrete way to construct $4d \mathcal{N} = 4$ super Yang-Mills theory by using the Eguchi-Kawai equivalence, which preserves 16 supersymmetries. Reference [22] studied the Eguchi-Kawai reduction in the strong coupling domain of $\mathcal{N} = 4$ super Yang-Mills by using AdS/CFT and D-branes.

³Recently, a new limiting procedure for the twisted Eguchi-Kawai model, which aims to prevent center breaking, has been proposed [23].

one on $T^3 \times S^1$ provided the $(\mathbb{Z}_N)^3$ center symmetry associated with the cycles on T^3 is not spontaneously broken. The phase transition in the thermodynamic $\mathbb{R}^3 \times S^1$ limit can be studied by using a large- N reduced model on small $T^3 \times S^1$ by dialing β . This form of equivalence is also useful for Hamiltonian formulation and extraction of the non-perturbative spectrum of the theory.

- (3) *Twisted QCD*: In compactified QCD(Adj), finite- N corrections turn out to be order $1/N$, as opposed to the perturbative expectation on \mathbb{R}^4 [35], which is order $1/N^2$. There are two plausibly related explanations for this behavior, whose footprints can be seen in finite-volume perturbation theory. In a weak-coupling center-symmetric background, the volume is only enhanced by a factor of N , and the effective volume is $V_{\text{eff}} \sim NV$. Finite- N corrections should scale as finite-volume corrections. The other is, in compact space, one cannot gauge away zero-momentum modes. Typically, there are order N bosonic and fermionic zero modes, which may generate nonperturbative $1/N$ effects [36]. Both problems can simultaneously be cured and $1/N$ corrections can systematically be improved by using twisted boundary conditions.⁴ We refer to the latter as TQCD(Adj) as per [15].

Our results have interesting spin-offs for noncommutative theories, phase transition in pure Yang-Mills theory, and orientifold equivalence. Adding massive or massless adjoint fermions to the twisted Eguchi-Kawai (TEK) model cures the global instability of the model [17–19]. Therefore, our formulation can be used to provide a non-perturbative definition of noncommutative bosonic Yang-Mills theory and noncommutative QCD(Adj). By using the reduced matrix model for TQCD(Adj) with very heavy adjoint fermions on $1^3 \times 2$ lattices, we observe the confinement/deconfinement transition at bare coupling $b_c = 0.32\text{--}0.33$. Large volume simulations for pure Yang-Mills theory give similar results, in accordance with the finite-temperature version of equivalence. [For example, $SU(8)$ YM theory simulated on $10^3 \times 5$ lattices gives, in the extrapolated infinite volume limit, $b_c \sim 0.34$ [40] (see also [41]). The small difference is due to $1/N$ effects, the existence of heavy fermions in our reduced model, and the difference of numbers of sites along the temporal direction.] We hope that the unitary matrix model can be used to gain insight into the nature of the deconfinement transition of the infinite volume theory.

⁴The relation between “effective” volume and N is discussed in many places (for a review, see [37]). The observations that twisted boundary conditions can be used (i) to systematically reduce finite-volume corrections is given in Ref. [38] and (ii) to lift bosonic and fermionic zero modes is given in Ref. [39]. We give analytic and numerical evidence suggesting that the two are indeed related.

Finally, combined with the large- N orientifold equivalence between (T)QCD(Adj) and QCD(AS), thermal properties of the QCD(AS) can also be studied by using the large- N reduced model for TQCD(Adj) at finite temperature [1,2,30].⁵ Our results for massive QCD(Adj) can be regarded as a first step towards this direction of research.

II REVIEW OF ORIGINAL EGUCHI-KAWAI PROPOSAL

In this section, we give a brief review of the Eguchi-Kawai equivalence. Our aim is not to repeat the original works on the subject; rather we wish to point out two important ingredients which will be useful. These are perturbative and nonperturbative quantum fluctuations in the matrix model.

The EK model is the dimensional reduction of Wilson’s lattice gauge theory action down to a 1^4 lattice, i.e., a one-site matrix model. The action of the reduced model is

$$S_{0d} = -2bN \text{Re Tr} \left(\sum_{\mu < \nu} V_{\mu} V_{\nu} V_{\mu}^{\dagger} V_{\nu}^{\dagger} \right), \quad (2)$$

where V_{μ} ($\mu = 1, 2, 3, 4$) are unitary matrices. b is the bare inverse ’t Hooft coupling constant. To probe continuum physics, b should be chosen appropriately depending on the lattice spacing a . This action has a $(\mathbb{Z}_N)^4$ global center symmetry

$$V_{\mu} \rightarrow e^{2\pi i n_{\mu}/N} V_{\mu}, \quad (n_{\mu} = 0, 1, \dots, N-1). \quad (3)$$

The reduced model (2) is equivalent to the translationally invariant subsector of the lattice theory with an arbitrary number of sites, provided center and translational symmetries are not broken. These are the necessary and sufficient symmetry realization conditions for the large- N volume independence.

A. Perturbative fluctuations and one-loop potential

The realization of center symmetry can be determined by integrating out weakly coupled perturbative modes in the background of diagonal, commuting Wilson lines:

$$V_{\mu} = \text{diag}(e^{i\theta_{\mu}^1}, \dots, e^{i\theta_{\mu}^N}), \quad [V_{\mu}, V_{\nu}] = 0. \quad (4)$$

The resulting one-loop action reads (we parallel the discussion in the one-site matrix model and continuum theory on small T^4)

⁵Earlier work on deconfinement transition in large- N QCD (Adj) and QCD(AS) in the weak-coupling limit of small $S^3 \times S^1$ showed that the critical temperatures agree [30], up to $1/N$ corrections.

$$S_{1\text{ loop}} = \begin{cases} 2 \sum_{a < b} \log \left[\frac{4}{a^2} \sum_{\mu=1}^4 \sin^2 \left(\frac{\theta_{\mu}^{ab}}{2} \right) \right] & \text{on } 1^4 - \text{lattice} \\ 2 \sum_{a < b} \sum_{\vec{k} \in \mathbb{Z}^4} \log \left(\sum_{\mu=1}^4 \frac{(2\pi k_{\mu} + \theta_{\mu}^{ab})^2}{L^2} \right) & \text{on } T^4 - \text{continuum,} \end{cases} \quad (5)$$

where $\theta_{\mu}^{ab} = \theta_{\mu}^b - \theta_{\mu}^a$. Note that the one-site matrix model and T^4 have the same symmetry properties, both invariant under $\theta_{\mu}^{ab} \rightarrow \theta_{\mu}^{ab} + 2\pi$.⁶ It is also convenient to rewrite (5) by using the Wilson lines. This can be done by a Fourier transformation for the former and by a Poisson resummation for the latter:

$$S_{1\text{-loop}}[V_1, \dots, V_4] = \begin{cases} \sum_{\vec{n} \in \mathbb{Z}^4 \setminus \{0\}} P(\vec{n}) (|\text{tr}(V_1^{n_1} \dots V_4^{n_4})|^2 - N) & \text{on } 1^4 - \text{lattice} \\ -\frac{1}{\pi^2} \sum_{\vec{n} \in \mathbb{Z}^4 \setminus \{0\}} \frac{1}{|\vec{n}|^4} (|\text{tr}(V_1^{n_1} \dots V_4^{n_4})|^2 - N) & \text{on } T^4 - \text{continuum,} \end{cases} \quad (6)$$

where

$$P(\vec{n}) = - \int \frac{d\alpha}{\alpha} e^{-8\alpha} I_{n_1}(2\alpha) \dots I_{n_4}(2\alpha), \quad (7)$$

and $I_n(2\alpha)$ is the modified Bessel function of the second kind; $I_n(2\alpha) = (2\pi)^{-1} \int_0^{2\pi} d\theta e^{2\alpha \cos(\theta)} e^{in\theta}$. In the one-site model, Fourier coefficients are slightly more complicated, but the main result is the same as in continuum T^4 . The basic point is the negative definiteness of the integral in (7). Moreover, at a large-winding number, the integral can be evaluated analytically by localization, and converges to the continuum T^4 result quickly:

$$\begin{aligned} P(\vec{n}) &\leq 0, \quad \forall \vec{n} \in \mathbb{Z}^4 \setminus \{0\}; \\ P(\vec{n}) &\approx -\frac{1}{\pi^2} \frac{1}{|\vec{n}|^4}, \quad \text{for } |\vec{n}| \gg 1. \end{aligned} \quad (8)$$

The one-loop action (5) has IR singularities whenever two (or more) eigenvalues coincide. This is also manifest in (6); both series are conditionally convergent at a large-winding number, and exhibit logarithmic divergence for coinciding eigenvalues. These issues are discussed thoroughly in the Appendix. Physically, at these points, there are extra massless degrees of freedom which should not have been integrated out. In other words, the zeroth order assumption that one can expand the fluctuations around commuting saddles (4) is not always correct. As discussed in the Appendix, the IR divergence can be regularized and meaningful results can be extracted from (5). The result is, of course, well-known; (5) generates an eigenvalue attraction, or in (6) the “masses” for Wilson lines are all negative and, consequently, eigenvalues clump. However, neither implies that all the eigenvalues are coincident. Because of non-perturbative effects, the eigenvalues spread. In order to estimate the size of the eigenvalue bunch, we may study the theory around one of its global minima, $V_{\mu} \approx 1$.

⁶The relation between the continuum one-loop effective action on T^4 and the one-loop effective action for the one-site theory given in Eq. (5) is analogous of the one between the action of the XY model and its Villain form.

B. Nonperturbative fluctuations and size of eigenvalue bunch

Parametrizing $V_{\mu} \approx e^{iaX_{\mu}}$, we observe that around the minimum of the one-loop potential, all the fluctuations are quartic (as opposed to being quadratic). The action expanded around one of the minima, the $V_{\mu} \approx 1$ configuration, gives

$$S_{0d} = \frac{N}{\lambda_{0d}} \text{Tr} \left(-\frac{1}{4} [X^{\mu}, X^{\nu}]^2 \right), \quad (9)$$

where

$$\lambda_{0d} = \begin{cases} \frac{1}{2ba^4} & \text{on } 1^4 - \text{lattice} \\ \frac{\lambda_{4d}(\frac{1}{L})}{L^4} \sim \frac{1}{\log(\frac{1}{L\Lambda})L^4} & \text{on } T^4 - \text{continuum,} \end{cases} \quad (10)$$

is the zero-dimensional 't Hooft coupling. In the lattice, b is, of course, a parameter that one can choose at will. However, to probe continuum physics, it needs to scale as $b \sim \log(1/a\Lambda)$ by asymptotic freedom.

Since the Hermitian matrix model is given in terms of noncompact matrices, it is not *a priori* guaranteed that the theory actually exists quantum mechanically. Reference [42] shows that the partition function of the theory defined through (9) does not exist for $SU(2)$, but exists for $SU(N)$ for $N \geq 3$. In the next section, we will indeed see closely related Hermitian matrix models which do not exist for any N . Despite this, the Hermitian matrix model defined through (9) is useful. It can be employed to determine the interaction between eigenvalues and to estimate the root-mean-square fluctuations of X_{μ} matrices. (We also refer to this as the size of the eigenvalue bunch.)

Scalar eigenvalues in $0d$ theory are related to the phases θ of the Wilson lines winding on temporal and spatial directions by

$$Lx_a^{\mu} = \theta_a^{\mu} \quad (a = 1, \dots, N). \quad (11)$$

The 't Hooft coupling λ_{0d} has the dimension of (mass)⁴ and its value sets the typical mass scale of the $0d$ theory (9). In particular, typical fluctuation of the eigenvalues of the dynamical fields is set by this scale. Because of the generic noncommutativity of X_{μ} matrices, the relative positions of

the eigenvalues make sense only when their separation is of order or larger than $\lambda_{0d}^{1/4}$ [34].

The one-loop effective action of the matrix model around the diagonal background can be calculated if all eigenvalue pairs are well-separated $|\tilde{x}_a - \tilde{x}_b| \gg \lambda_{0d}^{1/4}$, corresponding to the case where all eigenvalues are weakly coupled. Integrating out massive “ W bosons” (off-diagonal elements) by using the background field gauge yields

$$S_{1\text{-loop}}[x_{ab}^\mu] = 2 \sum_{a < b} \log |\tilde{x}_a - \tilde{x}_b|^2. \quad (12)$$

Clearly, this is nothing but Eq. (5) restricted to its Kaluza-Klein (KK) zero mode. Thus, as in the one-loop potential (5) of the full theory, the Hermitian model as well predicts eigenvalue attraction and also exhibits the same IR singularity whenever two eigenvalues coincide.

More importantly, the Hermitian matrix model (9) allows the determination of the typical size of eigenvalue fluctuations. In 't Hooft's large- N limit, the root-mean-square fluctuations ΔX are

$$\Delta X = \sqrt{\left\langle \frac{1}{N} \text{tr}(X_\mu^2) \right\rangle} \sim \lambda_{0d}^{1/4}. \quad (13)$$

This result has various interesting implications.

The analysis of the continuum T^4 and weak-coupling ($b \rightarrow \infty$) domain of lattice gauge theory exhibits similar behavior. Let $L = a$. Then, $\Delta X \sim 1/[\log(1/L\Lambda)]^{1/4} L < 1/L$. At asymptotically small L , the size of the eigenvalue bunch is much smaller than the size $2\pi/L$ of the dual torus where eigenvalues are residing. In this domain, clearly, nonperturbative fluctuations cannot overwhelm broken center symmetry.

It is well-known that Eguchi-Kawai reduction holds in the strong coupling domain of lattice gauge theory, for $0 \leq b < b_c = 0.19$. This is a lattice domain unrelated to continuum physics, whereas the above analysis is valid for sufficiently large b . What happens to ΔX if we decrease b to being of order few? Of course, this is unjustified, but demonstrates the trend of the root-mean-square fluctuations. Naive use of the $\Delta X \sim 1/b^{1/4}a$ shows that when $b^{1/4}$ is order one, the quantum fluctuations may be as large as the size of the dual torus. In this domain, eigenvalues feel the size of the compact space they live in and we expect the strong fluctuations to lead to center restoration. This is indeed the case.

In this paper, we will study Yang-Mills theory with massive adjoint fermions with mass m . When $m = \infty$, the discussion is the same as the original Eguchi-Kawai reduction. For $ma \sim \text{few}$, the perturbative-loop analysis indicates that only a finite subgroup of center symmetry would restore; however, such analysis does not take into account nonperturbative fluctuations. We propose that these fluctuations tend to uniformize the eigenvalue distribution rather quickly, even when $ma \sim \text{few}$, providing the resolution of the problem stated in the introduction.

III. EGUCHI-KAWAI EQUIVALENCE FOR MASSIVE QCD(Adj)

In this section we explain why it is natural to expect that the Eguchi-Kawai reduction holds for the QCD(Adj) with massive adjoint fermions at sufficiently small volume. Our analysis is based on the one-loop potential for diagonal components of fields and estimates of nonperturbative quantum fluctuations. We start with the zero temperature case and then generalize to the finite temperature.

A. QCD(Adj) at zero temperature on T^4 at small L

Let us consider the QCD(Adj) at zero temperature on a symmetric four-torus, with size L . At sufficiently small L , gauge coupling at the scale of the compactification is small and we may analytically compute the one-loop effective action on T^4 . The reason for doing this computation, apart from trying to determine the center-symmetry realization, is twofold. One is we would like to compare with the one-site theory, given in (31). More importantly, we give evidence that some (not all) implications of one-loop action are, in full theory, overwhelmed by large nonperturbative quantum fluctuations, and therefore, incorrect.

The one-loop effective action, in the Wilson line background (4), induced by gauge and fermionic fluctuations with periodic boundary conditions can be written as

$$S_{1\text{-loop}}[\theta_\mu^{ab}] = \sum_{a < b} \sum_{k_1, \dots, k_4} \left(2 \log \left(\sum_{\mu=1}^4 \frac{(2\pi k_\mu + \theta_\mu^{ab})^2}{L^2} \right) - 4N_f^D \log \left(\sum_{\mu=1}^4 \frac{(2\pi k_\mu + \theta_\mu^{ab})^2}{L^2} + m^2 \right) \right), \quad (14)$$

where $\theta_\mu^{ab} = \theta_\mu^a - \theta_\mu^b$, and m is the fermion mass. Similar to original EK model (5), this expression has IR singularities whenever two (or more) eigenvalues coincide, which we discuss thoroughly in the Appendix. The theory may have different saddles which are expressed in terms of noncommuting matrices. The classification of the saddles, using the techniques of Ref. [43], of QCD(Adj) as a function of mass of the fermion is given in the Appendix.

When we consider a regime where $|\vec{\theta}^{ab}| \ll 2\pi$, we can split (14) into the zero and non-zero-momentum contribution. The eigenvalue dynamics is dominated by the interactions between nearby eigenvalues and the effect of high KK modes is negligible. Therefore, we will use the truncated Hermitian matrix model (15) to gain an understanding of the typical eigenvalue fluctuations. Strictly speaking, the truncation can be justified only when the $(\mathbb{Z}_N)^4$ center symmetry is completely broken and consequently there exists a clear separation of scales between the KK modes and zero modes. In a center-symmetric background, this is not the case. However, at large- N , the states obtained by quantizing the theory on a center-symmetric vacuum fill the $[0, 2\pi/L]$ energy range uniformly. If we consider a finite but small range $|\vec{\theta}^{ab}| \ll 2\pi$, there are still $O(N^2)$

states (in perturbation theory) in this interval. We may therefore use the Hermitian model to probe the interaction of nearby eigenvalues, and their fluctuations. The eigenvalue dynamics of the full theory is mimicked rather accurately by the truncated Hermitian matrix model.

The truncation of the KK modes in (1) yields the zero-dimensional Hermitian matrix model⁷

$$S_{0d} = \frac{N}{\lambda_{0d}} \text{Tr} \left(-\frac{1}{4} [X^\mu, X^\nu]^2 + \sum_{f=1}^{N_f^D} \bar{\psi}_f (\gamma_\mu [X^\mu, \psi_f] + m \psi_f) \right), \quad (15)$$

where $\lambda_{0d} = \lambda_{4d}(1/L)/L^4 \sim 1/\log(1/L\Lambda)L^4$ is the zero-dimensional 't Hooft coupling, and Λ is the strong scale of QCD(Adj).

The $\lambda_{0d}^{1/4}$ and m are the two scales in the Hermitian matrix model (15). In particular, for the $m = \infty$ theory, which corresponds to the original EK model discussed in Sec. II, the root-mean-square fluctuations of matrices are set by this scale $\Delta X(m = \infty) \sim \lambda_{0d}^{1/4}$. With standard 't Hooft scaling, this is $O(N^0)$ in the large- N limit. This is a crucial observation that will be important below. Because of the generic noncommutativity of X_μ matrices, the relative positions of the eigenvalues make sense only when their separation is of order or larger than $\lambda_{0d}^{1/4}$ [34].

The one-loop effective action of the matrix model around the diagonal background can be calculated if all eigenvalue pairs are well-separated $|\vec{x}_a - \vec{x}_b| \gg \lambda_{0d}^{1/4}$, corresponding to the case where all eigenvalues are weakly coupled. Integrating out massive “ W bosons” (off-diagonal elements) by using the background field gauge yields

$$S_{1\text{ loop}}[x_{ab}^\mu] = 2 \sum_{a < b} \log |\vec{x}_a - \vec{x}_b|^2 - 4N_f^D \sum_{a < b} \log (|\vec{x}_a - \vec{x}_b|^2 + m^2). \quad (16)$$

Note that this is nothing but Eq. (14) restricted to its KK zero mode, as expected.

The effect of adjoint fermions, which is most manifest in (16), is to generate repulsion among eigenvalues. At $m = \infty$, since the fermions do not contribute, they have no impact on ΔX . For finite fermions' mass, the effect of fermions makes ΔX larger than that of the $m = \infty$ case. Although we will not prove this statement, it is easy to understand it on physical grounds. When fermion mass is

zero, then the one-loop potential is unbounded from below only at *large* eigenvalue separation; hence $\Delta X(m = 0) = \infty$. From now on, we assume $\Delta X(m) \geq \Delta X(m = \infty) = \lambda_{0d}^{1/4}$. Somewhat conservatively, we use the smaller of the fluctuations in what follows.

Let us now discuss the realization of $(\mathbb{Z}_N)^4$ symmetry based on the effective action (16) for the Hermitian matrix model.

1. $N_f^D = 0$ (bosonic)

The $N_f = 0$ or $m = \infty$ limits are the same and are discussed in Sec. II. We repeat the main result for convenience. The one-loop action leads to the mutual attraction of eigenvalues at large eigenvalue separation, and hence, eigenvalues must clump. This implies broken center symmetry. However, at small eigenvalue separation, one-loop approximation is not valid; the background of the commuting Wilson line saddles breaks down. Because of nonperturbative quantum fluctuations, the eigenvalues do not collapse to a point; rather the eigenvalue clump has a finite extent of the order $\Delta X \sim \lambda_{0d}^{1/4} \equiv [\lambda_{4d}(1/L)]^{1/4}/L$. Note that, although the size of the eigenvalue clump is suppressed with respect to $1/L$ at small $\lambda_{4d}(1/L)$ and hence center symmetry is broken, it scales as $O(N^0)$ in the large- N limit. This will be crucial later.

2. $N_f^D = 1/2$ (single Majorana)

When $N_f^D = 1/2$ and $m = 0$, the theory is $4d$ $\mathcal{N} = 1$ pure super Yang-Mills theory. In this case, the one-loop effective action (16) vanishes, and in fact, this is true to all loop orders due to supersymmetry. Taking nonperturbative fractional instanton effects into account, the center is unbroken on $\mathbb{R}^3 \times S^1$ as discussed in [7]. In supersymmetric theories with supersymmetry preserving boundary conditions, it is expected that there are no phase transitions as the volume is varied [39]. At large- N , the absence of phase transitions transmutes to exact volume independence [7] and unbroken $(\mathbb{Z}_N)^4$ center symmetry. However, it is also possible to construct a metastable center-broken sector [44], which becomes stable at large- N .

When m is fixed and nonzero, by taking $L \rightarrow 0$, (16) is positive, and therefore, $(\mathbb{Z}_N)^4$ symmetry breaks down. If L is fixed and $m \rightarrow 0$, a center-symmetry preserving background exists for a finite range of m . This aspect is discussed thoroughly in Ref. [45]. This noncommutativity of limits requires care in drawing conclusions about this case.

3. $N_f^D \geq 1$: Uniformization of eigenvalue distribution

The effective action (16) predicts attraction at short distance $|\Delta x| \lesssim m$, and repulsion at long distance $|\Delta x| \gtrsim m$. Then one may naively conclude that all eigenvalues clump and $(\mathbb{Z}_N)^4$ symmetry is broken. However, one should notice that this effective action is valid only at

⁷It should be understood that the Hermitian model (15) is used as an auxiliary. In the strict $L = 0$ limit, and for massless fermions, the partition function of the Hermitian model diverges. One-loop potential is unbounded from below as eigenvalue separations tend to infinity. At finite- L , the target space of eigenvalues is bounded, it cannot run off to infinity, and the partition function of the finite- L theory exists.

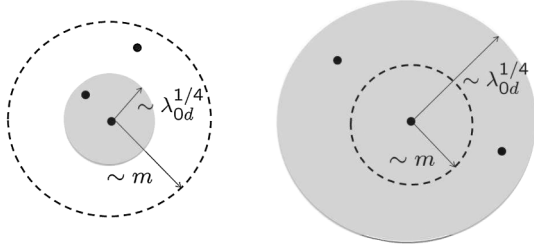


FIG. 1. The scales in the problem. Left panel: $m \gtrsim \lambda_{0d}^{1/4}$ and mass is important. Right panel: $m \lesssim \lambda_{0d}^{1/4}$ and mass is negligible with respect to quantum fluctuations. We can always realize the latter case by taking the size of the four-torus sufficiently small, but still $O(N^0)$. See the text for explanations.

$|\Delta x| \gtrsim \lambda_{0d}^{1/4}$. When $\lambda_{0d}^{1/4} \lesssim m$ attractive force emerges at $\lambda_{0d}^{1/4} \lesssim |\Delta x| \lesssim m$, and hence $(\mathbb{Z}_N)^4$ is broken (left of Fig. 1). When $\lambda_{0d}^{1/4} \gtrsim m$, however, it predicts only repulsion; eigenvalue fluctuation is of order $\lambda_{0d}^{1/4}$ and hence they cannot clump to a small region where (16) predicts attraction (right of Fig. 1).

At sufficiently small, but $O(N^0)$ compactification radii L , we can always guarantee that nonperturbative quantum fluctuations overwhelm fermion mass, i.e., $\lambda_{0d}^{1/4} \equiv [\lambda_{4d}(1/L)]^{1/4}/L \gtrsim m$. In this case, fermion mass is negligible and for the purpose of center-symmetry realization, the theory cannot be distinguished from the massless theory, for which center symmetry is unbroken. At such values of L , since the target space of eigenvalues is compact four-torus \tilde{T}^4 with size $\frac{1}{L}$, the repulsion implies that the eigenvalues will uniformly distribute over \tilde{T}^4 .

This is the sense in which lower dimensional nonperturbative quantum fluctuations help restoration of center symmetry at $mL \sim \text{few}$, as opposed to quantum field theory on $\mathbb{R}^3 \times S^1$ where full center restoration requires $mLN \sim \text{few}$.

As we will see in the Appendix, the $(\mathbb{Z}_N)^4$ broken phase which consists of k bunches of eigenvalues may exist when $(\lambda_{0d}/k)^{1/4} \ll m$. However, the radius of each bunch is of order $(\lambda_{0d}/k)^{1/4}$, which is smaller than the eigenvalue fluctuation in the $(\mathbb{Z}_N)^4$ symmetric phase $(\lambda_{0d})^{1/4}$, and hence even if the $(\mathbb{Z}_N)^4$ broken phase exists, tunneling to such a state is highly suppressed.

The above argument explains the reason for the working of Eguchi-Kawai reduction in Refs. [32,33] for heavy fermions. In [32], initial configuration for simulation corresponds to $X^\mu = 0$ (single bunch). It is unstable and collapses to the $(\mathbb{Z}_N)^4$ symmetric phase.

B. QCD(Adj) at finite temperature on asymmetric $T^3 \times S^1$

We can generalize the argument of the previous subsection to the finite-temperature QCD(Adj) on an asymmetric

four-torus $T^3 \times S^1$. Circumferences of temporal and three spatial circles are taken to be β and L . On fermions, we impose antiperiodic and periodic boundary conditions along temporal and spatial circles, respectively.

Completely analogous to the discussion of Sec. III A, at small L , the eigenvalue dynamics of the full theory is mimicked rather accurately by the truncated Hermitian matrix quantum mechanics with action:⁸

$$S_{1d} = \frac{N}{\lambda_{1d}} \int_0^\beta dt \text{Tr} \left(\frac{1}{2} (D_t X^i)^2 - \frac{1}{4} [X^i, X^j]^2 + \sum_{a=1}^{N_f^D} \bar{\psi}_a (\gamma^0 D_t \psi_a + \gamma_i [X^i, \psi_a] + m \psi_a) \right), \quad (17)$$

where

$$\lambda_{1d} = \frac{\lambda_{4d}}{L^3}. \quad (18)$$

The 't Hooft coupling λ_{1d} has the dimension of (mass)³ and its value sets the typical mass scale of the theory. In particular, typical fluctuation of the eigenvalues of the dynamical fields is given by this scale. The mapping between the scalar eigenvalues and the phases θ of the Wilson loops is the same as in (11), but now only running over spatial directions. Since the S^1 direction is compact, unlike its decompactification limit $S^1 \rightarrow \mathbb{R}$, the Wilson line along that direction cannot be gauged away. We parametrize $W_t = \text{diag}(e^{i\alpha_1\beta}, \dots, e^{i\alpha_N\beta})$, or $A_t = -i\beta^{-1} \log W_t$.

The one-loop effective action of the matrix quantum mechanics around the static diagonal background in the background field gauge can be computed in the weak-coupling domain,

$$\frac{\lambda_{1d}^{1/3}}{|\vec{x}_a - \vec{x}_b|} \ll 1 \quad \text{or} \quad \lambda_{1d}^{1/3} \beta \ll 1, \quad (19)$$

resulting in

$$S_{1d,1 \text{ loop}}(\alpha, \vec{x}) = 2 \sum_{a < b} \sum_{n=-\infty}^{\infty} \log \left(\left(\frac{2\pi n}{\beta} + (\alpha_a - \alpha_b) \right)^2 + |\vec{x}_a - \vec{x}_b|^2 \right) - 4N_f^D \sum_{a < b} \sum_{n=-\infty}^{\infty} \log \left(\left(\frac{2\pi(n+1/2)}{\beta} + (\alpha_a - \alpha_b) \right)^2 + |\vec{x}_a - \vec{x}_b|^2 + m^2 \right), \quad (20)$$

where α_a and \vec{x}_a represent diagonal components of the gauge field A_t and three scalars X_i , respectively.

⁸We repeat the same cautionary note as in Sec. III A. The classical theory written in Eq. (17) does not exist as a quantum theory. In the strict $L = 0$ limit, and for massless fermions (or fermions with a finite mass), the theory does not have a ground state. In this paper, we study the finite- L , $N \rightarrow \infty$ limit of (1) which is a well-defined quantum theory. The Hermitian model (17) will be useful as an auxiliary to infer some general lessons about the finite- L case.

By subtracting a constant factor, (20) can be rewritten as [46] (for reference, we quote both periodic and antiperiodic boundary conditions along β circle)

$$S_{1d,1\text{ loop}}^\pm = 2 \sum_{a<b} \log(\cosh(\beta|\vec{x}_a - \vec{x}_b|) - \cos(\beta(\alpha_a - \alpha_b))) - 4N_f^D \sum_{a<b} \log(\cosh(\beta\sqrt{|\vec{x}_a - \vec{x}_b|^2 + m^2}) \mp \cos(\beta(\alpha_a - \alpha_b))). \quad (21)$$

From the expression of $S_{1d,1\text{ loop}}^-$, one might naively conclude that eigenvalues \vec{x}_a and α_a coincide, because the one-loop action is negative infinity at that point. However, the analysis is valid only when condition (19) is satisfied; thus drawing reliable conclusions requires care.

The $\beta \rightarrow \infty$ limit of (21) is both intuitive and insightful. Since it is the limit of arbitrarily low temperatures, the fermionic boundary conditions should not matter, and indeed, this is transparent from (21); the hyperbolic cosine increases unboundedly, and the trigonometric cosine is bounded, and hence the one-loop expression is dominated by the former.⁹ The ground-state energy of the system at one-loop order (or one-loop potential) can be deduced from the limit $\lim_{\beta \rightarrow \infty} S_{1d,1\text{ loop}}/\beta \equiv E_{1d,1\text{ loop}}[|\vec{x}_{ab}|]$ and the result is

$$E_{1d,1\text{ loop}}[|\vec{x}_{ab}|] = 2 \sum_{a<b} |\vec{x}_a - \vec{x}_b| - 4N_f^D \sum_{a<b} \sqrt{|\vec{x}_a - \vec{x}_b|^2 + m^2},$$

$$\lim_{m \rightarrow 0} E_{1d,1\text{ loop}}[|\vec{x}_{ab}|] = (2 - 4N_f^D) \sum_{a<b} |\vec{x}_a - \vec{x}_b|. \quad (22)$$

This is an intuitive and simple result¹⁰ and various remarks are in order regarding the chiral ($m = 0$) limit on \mathbb{R} .

- (1) For $N_f^D > 1/2$, $E_{1d,1\text{ loop}}[|\vec{x}_{ab}|]$ is unbounded from below and eigenvalues mutually repel each other.

⁹Also note that at the $\beta \rightarrow \infty$ limit, A_i can be gauged away. Hence, it should not appear in the one-loop potential.

¹⁰We could have guessed this result by physical reasoning as follows: In the weak-coupling domain where $\lambda_{1d} = \lambda_{1d}/|\vec{x}_{ab}|^3 \ll 1$ is small and one-loop analysis is reliable, the Lagrangian (17) reduces to a collection of bosonic and fermionic harmonic oscillators:

$$L \approx \frac{1}{2} |\partial_t \vec{X}^{ab}|^2 + \frac{1}{2} |\vec{x}_a - \vec{x}_b|^2 |\vec{X}^{ab}|^2 + \text{fermionic oscillators}.$$

The eigenvalue differences of background \vec{X} matrices are identified with the frequencies of harmonic oscillators, $\omega_{ab}^b = |\vec{x}_a - \vec{x}_b|$ and $\omega_{ab}^f = \sqrt{|\vec{x}_a - \vec{x}_b|^2 + m^2}$. In the chiral limit, $\omega_{ab}^f = \omega_{ab}^b$. In gauge quantum mechanics, there are $2\sum_{a<b}$ many massive bosonic fluctuations and $2 \times 2N_f^D \sum_{a<b}$ many massive fermionic fluctuations. Hence, the background dependence of the ground-state energy of the system is

$$E = \sum_{\text{bosons}} \frac{1}{2} \omega^b - \sum_{\text{fermions}} \frac{1}{2} \omega^f = E_{1d,1\text{ loop}}[|\vec{x}_{ab}|],$$

which is given in (22).

The classical minima corresponding to the space of commuting triples $[X_i, X_j] = 0$ are unstable against perturbative quantum fluctuations. This means, at the $L = 0$ limit, the Hermitian matrix quantum mechanics (17) does not have a ground state.

- (2) At finite L , since the target space of eigenvalues is compact three-torus \tilde{T}^3 with size $1/L$, the repulsion implies that eigenvalues will uniformly distribute over \tilde{T}^3 . This implies unbroken center symmetry in the $N = \infty$ limit and the theory obeys volume independence.
- (3) For $0 \leq N_f^D < 1/2$, $E_{1d,1\text{ loop}}[|\vec{x}_{ab}|]$ is bounded from below. The minimum is at $|\vec{x}_{ab}| = 0$. However, in this domain, one-loop analysis is not reliable, and there are quantum fluctuations of order $\lambda_{1d}^{1/3}$. At $N_f^D = 1/2$, $m = 0$, the ground-state energy is zero to all orders in perturbation theory due to supersymmetry.

In the following, we study in more detail the phase structure of the four-dimensional theory by using (21) and estimates of the nonperturbative quantum fluctuations. We first explain $N_f^D = 0$ (bosonic) and $N_f^D = 1/2$ (or one Majorana fermion) cases. We then study the case with $N_f^D \geq 1$, our main interest in this paper.

1. $N_f^D = 0$ (bosonic)

The one-loop action (21) generates an attraction between eigenvalues at long distance and the center symmetry is broken. More precisely, there are N^3 saddles related to each other by center conjugations. The tunneling between these saddles is suppressed in the large- N limit and the theory is in a center-broken phase. However, the eigenvalues do not collapse to a single point due to the nonperturbative quantum fluctuations; the clump has a finite size of order $\lambda_{1d}^{1/3} \equiv [\lambda_{4d}(1/L)]^{1/3}/L$ which is $O(N^0)$ in the large- N limit.

2. $N_f^D = 1/2$ (single Majorana)

The supersymmetric theory ($N_f^D = 1/2$ and $m = 0$) has been studied extensively, because its maximally supersymmetric cousin has a dual description as the D0-brane system. In this case the one-loop potential falls off exponentially,

$$S_{1d,1\text{ loop}}^- \sim \sum_{a<b} \exp(-\beta|\vec{x}_a - \vec{x}_b|), \quad (23)$$

and the ground-state energy is $E_{1d,1\text{ loop}}[|\vec{x}_{ab}|] = \lim_{\beta \rightarrow \infty} S_{1d,1\text{ loop}}^-/\beta \rightarrow 0$. This follows from the cancellation of the attractions and repulsions between eigenvalues due to supersymmetry. Consequently, there exists a space of flat directions. Therefore, once eigenvalues are well separated, they will propagate freely like the gas of D0-branes to all order in perturbation theory.

In order to study nonperturbative aspects, it is more useful in this case to recall that the theory is formulated on $T^3 \times \mathbb{R}$, and to discuss the system in Hamiltonian formulation. As asserted above, to all orders in perturbation theory, the theory has a moduli space, and all possible realizations of center symmetry are possible. However, nonperturbatively, this is not the case. Quantization of the zero-momentum bosonic modes gives rise to a discrete spectrum and a gap.

Witten studied the gauge quantum mechanics for finite- N within Born-Oppenheimer approximation and showed that the bosonic ground-state wave function (ignoring fermionic zero modes which are not crucial in what follows) is constant

$$\Psi_0(\vec{\theta}_1, \dots, \vec{\theta}_{N-1}) = 1 \quad (24)$$

and the excited states have an energy gap [39]. The center symmetry and volume independence was not discussed in Ref. [39]; however, its results have natural implications which apply to our discussion. In particular, we can introduce an eigenvalue distribution function $\rho(\vec{\theta})$ measuring the density of eigenvalues. The density is everywhere non-negative and obeys $\int d^3\vec{\theta} \rho(\vec{\theta}) = 1$. Since the ground-state wave function spreads uniformly over the perturbative flat directions,

$$\rho(\vec{\theta}) = \frac{1}{(2\pi)^3}, \quad (25)$$

and the center is unbroken. Unlike the discussion in Sec. III B 1, it is also unbroken at large- N . Nonperturbatively, we have a unique saddle singlet under center conjugations, and this is the main difference with respect to purely bosonic theory which has N^3 saddles.

When the fermion is massive, there is a subtlety due to the order of limits of small mass vs small- L analogous to the discussion in Sec. III A 2, with similar conclusions.

Finally, at large- N , this theory has a metastable bound state of eigenvalues [44] (with diverging lifetime as $N \rightarrow \infty$) which is analogous to the one in maximally supersymmetric theory [47] corresponding to the black zero-brane in type IIA supergravity.

3. $N_f^D \geq 1$

First consider the case with $m = 0$. From the one-loop effective action (21), it is apparent that repulsive force coming from fermions dominates at long distance. In the limit where T^3 is shrunk to zero size, the resulting Hermitian quantum matrix model is not well defined; the one-loop potential is unbounded from below for large eigenvalue separations. For finite $T^3 \times \mathbb{R}$, the eigenvalues can no longer run off to infinity; instead they spread over the dual \tilde{T}^3 uniformly. We expect the center-symmetric phase to continue upon compactification, down to $T^3 \times S^1_\beta$ so long as $\lambda_{1d}^{1/3} \beta \gg 1$. In this domain, the center symmetry is intact, and in the large- N limit, volume independence must hold.

In the high temperature limit, $\lambda_{1d}^{1/3} \beta \ll 1$, fermions decouple due to thermal mass, eigenvalues clump, and a metastable bound state of eigenvalues exists. Let us assume $|\beta\Delta x|, |\beta\Delta\alpha| \ll 1$, where $\Delta x = \max_{a,b}\{|\vec{x}_a - \vec{x}_b|\}$ and $\Delta\alpha = \max_{a,b}\{|\alpha_a - \alpha_b|\}$. Then the second term in the right-hand side of (21) is negligible, due to the large thermal mass of fermions, and the effective action becomes that of the zero-dimensional bosonic matrix model,

$$S_{1d,1\text{ loop}}^- \sim S_{0d,\text{bos}}[x_a^\mu] = 2 \sum_{a < b} \log |\vec{x}_a - \vec{x}_b|^2, \quad (26)$$

where we used the identification $x_a^4 = \alpha_a$. This potential produces attraction between eigenvalues. This model is studied extensively, and taking into account nonperturbative effects, a bound state of eigenvalues exists and it satisfies conditions $|\beta\Delta x|, |\beta\Delta\alpha| \ll 1$. In this domain, $(\mathbb{Z}_N)^4$ center symmetry is completely broken.

Generalization to nonzero m is straightforward and follows from the discussion of Sec. III A 3 on T^4 . At sufficiently small $O(N^0)$ volume such that $m \ll \lambda_{1d}^{1/3}$, the effect of mass is small, and hence attraction in one-loop action is overwhelmed by nonperturbative quantum fluctuations. In this domain, the $(\mathbb{Z}_N)^3$ center symmetry is intact.

IV. LATTICE MODEL AND MONTE CARLO SIMULATION

In Sec. III A, we explained on continuum T^4 and $T^3 \times S^1$ why the Eguchi-Kawai reduction holds for the QCD(Adj) at zero and finite temperature, based on perturbative-loop analysis, supplemented crucially with the estimates of nonperturbative quantum fluctuations. Below, we study the unitary matrix model and one-dimensional lattice model by using Monte Carlo simulation.

It is hard to implement the thermal model on a computer since the temporal direction is not reduced. Moreover, in order to describe phenomena typical to the finite-temperature system, we need to take the effective spatial volume¹¹ sufficiently large compared to N_t . As for a lattice model with an isotropic lattice spacing, roughly speaking, we need to take the spatial lattice size N_s to be twice larger than the temporal one N_t , $N_s \gtrsim 2N_t$. Since the N_s^{eff} is related to the matrix size N for the large- N reduced models

¹¹The space size in its ordinary sense is fixed. By developing perturbation theory around a center-symmetric background, say, for simplicity with only one-dimension compact, we observe that both the lowest states and the spacing between the states is suppressed by a factor of N and is given by $2\pi/(LN)$ as opposed to the usual (center-broken) KK spectrum where the level spacing is $2\pi/L$. In other words, to all orders in perturbation theory, the effective space size is enhanced into $L_{\text{eff}} = LN$. [See the discussion in [26] for QCD(Adj) and related discussions in a review [37] for quenched Eguchi-Kawai model (QEK) and TEK.] This is the perturbative essence of volume independence, and in the sense of neutral sector observables, the decompactification limit can be reached at $N \rightarrow \infty$ while keeping L fixed.

in the sense described in footnote 11, we need to take N large enough to satisfy this condition. When we use the original Eguchi-Kawai reduction for the spatial directions, finite- N correction behaves as $1/N$ rather than $1/N^2$, as we will show numerically. This fact indicates that the effective lattice size scales as $N_s^{\text{eff}} \sim N^{1/3}$, and it is not practical for numerical simulations. Therefore, to gain more effective spatial volume, we impose a twisted boundary condition on the spatial directions. For the latter, the effective volume is more enhanced, and volume independent domain can be reached more quickly. We call the QCD(Adj) with the twisted boundary condition as TQCD(Adj). The introduction of TQCD(Adj), which is algorithmically more convenient, is our main improvement over the one-site model of Ref. [32].

To explain the efficiency of the TQCD(Adj), we start with the zero temperature case, that is, the single-site model with a periodic boundary condition along the temporal direction on fermions. Then we apply the twist to the finite-temperature case, that is, the one-dimensional lattice model with an antiperiodic boundary condition on fermions along the temporal direction, and then see the Eguchi-Kawai reduction holds in this case. Especially we show this reduced model at finite temperature describes the confinement/deconfinement transition.

A. Single-site theories

1. QCD(Adj) on 1^4 lattice

The single-site matrix model can be obtained from a four-dimensional lattice gauge theory by reducing the number of lattice sites to one in all directions [32]. The action is

$$S_{0d} = -2bN \text{Re Tr} \left(\sum_{\mu < \nu} V_\mu V_\nu V_\mu^\dagger V_\nu^\dagger \right) + S_F, \quad (27)$$

where V_μ ($\mu = 1, 2, 3, 4$) corresponds to the link variable in the four-dimensional theory. The inverse 'tHooft coupling constant b should be chosen appropriately depending on the lattice spacing a . The fermionic part S_F is obtained as a dimensional reduction of the Wilson-Dirac fermion term

$$S_F = \sum_{f=1}^{N_f^D} \left(\bar{\psi}_f \psi_f - \kappa \sum_{i=1}^3 \{ \bar{\psi}_f (1 - \gamma_\mu) V_\mu \psi_f V_\mu^\dagger + \bar{\psi}_f (1 + \gamma_\mu) V_\mu^\dagger \psi_f V_\mu \} \right). \quad (28)$$

The hopping parameter κ can be expressed as

$$\kappa = \frac{1}{8 + 2am_0}, \quad (29)$$

where m_0 is the bare mass.

This action has a $(\mathbb{Z}_N)^4$ center symmetry

$$V_\mu \rightarrow e^{2\pi i n_\mu / N} V_\mu \quad (n_\mu = 0, 1, \dots, N-1). \quad (30)$$

If this symmetry is not broken, then the model is equivalent to the translationally invariant subsector of lattice theory with an arbitrary number of sites, including an infinite lattice limit.

Although detailed analytic evaluation of one-loop effective potential depends on the choice of lattice fermions,¹² intuitively, the absence of the center-symmetry breaking phase follows closely the discussion on continuum T^4 . The discussion on T^4 can easily be generalized to the 1^4 lattice. The role of the compactification scale L is replaced by the lattice spacing a in the one-site model. The main lesson that we learn is that the center symmetry on the 1^4 lattice model is in fact much more robust than the center on continuum T^4 .

The one-loop action for the one-site theory in the classical background of commuting Wilson lines $[V_\mu, V_\nu] = 0$ where $V_\mu = \text{diag}(e^{i\theta_\mu^1}, \dots, e^{i\theta_\mu^N})$ is given by

$$S_{1\text{ loop}} = 2 \sum_{a < b} \log \left[\frac{4}{a^2} \sum_{\mu=1}^4 \sin^2 \left(\frac{\theta_\mu^{ab}}{2} \right) \right] - 4N_f^D \sum_{a < b} \log \left(\frac{1}{a^2} \sum_{\mu=1}^4 \sin^2 \theta_\mu^{ab} + \left(m_0 + \frac{2}{a} \sum_{\mu=1}^4 \sin^2 \left(\frac{\theta_\mu^{ab}}{2} \right) \right)^2 \right). \quad (31)$$

The first term is induced by gauge fluctuations and leads to eigenvalue attraction [13]. Geometrically,

$$\mathcal{P}_\mu^{ab} \equiv \frac{2}{a} \left| \sin \left(\frac{\theta_\mu^a - \theta_\mu^b}{2} \right) \right| = \frac{2}{a} |e^{i\theta_\mu^a} - e^{i\theta_\mu^b}| \quad (32)$$

is the separation between two eigenvalues of the Wilson line in the μ direction. $\mathcal{P}^2 \equiv \sum_{\mu=1}^4 (\mathcal{P}_\mu^{ab})^2$ is the spectrum of massive gauge fluctuations (W bosons), familiar from the usual D -brane pictures as the spectrum of open strings ending on branes, where eigenvalues of the Wilson line are identified with branes. The second term, proportional to N_f^D , is induced by fermionic fluctuations, and is equal to $-4N_f^D \sum_{a < b} \log[M_f^2[\theta_\mu^{ab}]]$ where $M_f^2[\theta_\mu^{ab}]$ is the spectrum of fermions.

Equation (31) may be rewritten in a form mimicking the continuum expression on T^4 given in (14):

$$S_{1\text{ loop}}[\theta_\mu^{ab}] = 2 \sum_{a < b} \log \left[\sum_{\mu=1}^4 (\mathcal{P}_\mu^{ab})^2 \right] - 4N_f^D \sum_{a < b} \log \left[\sum_{\mu=1}^4 (\mathcal{P}_\mu^{ab})^2 + \sum_{\mu < \nu} \frac{a^2 (\mathcal{P}_\mu^{ab})^2 (\mathcal{P}_\nu^{ab})^2}{2(1 + m_0 a)} + \frac{m_0^2}{(1 + m_0 a)} \right], \quad (33)$$

¹²Here, we use the Dirac-Wilson fermion with Wilson parameter $r = 1$; [33] uses overlap fermions, and also discusses naive fermions.

where we have subtracted a holonomy-independent constant term. This expression can be Poisson resummed and be written in terms of Wilson lines as

$$S_{1\text{ loop}}[\theta_\mu^{ab}] = \sum_{a < b} \sum_{\vec{n} \in \mathbb{Z}^4 \setminus \{0\}} e^{i\vec{\theta}^{ab} \cdot \vec{n}} P_{\vec{n}}(m_0 a), \quad (34)$$

as discussed in the Appendix. The only difference with respect to the continuum expression on T^4 is that

$$P_{\vec{n}}^{\text{1site}}(0) = e_{\vec{n}} P_{\vec{n}}^{T^4}(0), \quad (35)$$

where $e_{\vec{n}}$ is an enhancement factor of a one-site model over continuum T^4 , for both bosonic and fermionic contribution. In general, due to peculiarities of the dispersion relation of the one-site model, the center stability is further enhanced on the one-site model with respect to continuum T^4 . Asymptotically, for $|\vec{n}| \gg 1$, $e_{\vec{n}} \rightarrow 1$ as expected on physical grounds, by just inspecting the dispersion relations.

The fermionic contribution to $e_{\vec{n}}$ is numerically sizeable and has interesting implications. For example, on T^4 , start with $mL = \infty$. Following the discussion of the Appendix, the singly-winding Wilson lines do get stabilized (in perturbation theory) at $mL = 2.027$, whereas for the one-site model, the same phenomena take place at $m_0 a = 9.3$. This is due to the fact that in the domain of heavy fermion bare mass, the last term in (33), which may roughly be viewed as an “effective mass” m_{eff}^2 , is suppressed with respect to the bare mass, $m_{\text{eff}} \sim \sqrt{m_0/a}$. For $N_f^D = 1$ theory, the fermions’ contribution dominates, leading to eigenvalue repulsion, and unbroken center symmetry for the theory defined on a 1^4 lattice, or EK reduction of QCD(Adj) to a single-site lattice.

If one-loop perturbation theory was the whole description, this would be the transition to a $(\mathbb{Z}_2)^4$ restored phase. However, as explained above, many phases can coexist and it is beyond perturbation to determine which phase is chosen in the end. Interestingly, the point where the center symmetry (partially) restores in simulation is very close to the prediction by perturbation theory $\kappa \approx 0.037$. This is approximately the value of κ where Ref. [32] observed the full center restoration, not just \mathbb{Z}_2 . In Fig. 4, we can also see the restoration around the same value. Although we could not see partial breaking clearly by measuring the observable employed in Ref. [32], the discrepancy between $\langle |W| \rangle$ in large- κ start and the one in small- κ start may indicate the existence of a partial breaking phase.

2. TQCD(Adj) at zero temperature

In compactified QCD(Adj), as we will see explicitly from simulations, the finite- N corrections turn out to be order $1/N$, as opposed to the perturbative expectation on \mathbb{R}^4 [35]. As explained in the results section of Sec. I, there are two plausibly related explanations for this behavior. One is related to the discussion of effective volume in the

reduced model. In the reduced model, N serves the role of an emergent spacetime volume, at least in a perturbative description in finite volume around a center-symmetric configuration. Finite- N corrections should scale as finite-volume corrections. However, what is not always clear is the factor N^p via which volume enhancement takes place $V_{\text{eff}} \sim N^p V$,¹³ and p may in fact be determined nonperturbatively.

In compact space, one cannot gauge away zero-momentum modes, and these modes are crucial in studying perturbation theory in finite volume. In perturbation theory, the spectrum of the theory relies on the background for the Wilson lines. If theory has massless adjoint fermions, there will also be fermionic zero modes in the spectrum. Typically, there are order N light or massless bosonic and order N fermionic zero modes, which may generate nonperturbative $1/N$ effects [36].

Both problems can simultaneously be solved and $1/N$ corrections can systematically be improved by using boundary conditions which cannot be obeyed by either bosonic or fermionic (if there are any) zero modes. This can be done by using the twisted boundary conditions of ’t Hooft [48]. This idea is, of course, not new, and is used by Witten in Ref. [39] to lift the zero modes in $\mathcal{N} = 1$ super Yang Mills theory in the context of supersymmetric theories on $T^3 \times \mathbb{R}$, and by Gonzalez-Arroyo and Okawa [15] in the context of large- N reduced models.

Our main observation can be summarized by using the following pedagogical exercise. (The generalization to the theories that we use in simulations is straightforward. The prescription given below works equally well on lattice and continuum.) Let $\Phi(x_1, x_2, x_3, x_4)$ denote either a unitary gauge field or an adjoint fermion field. We impose the following generalized boundary conditions on fields

$$\Phi(\dots, x_\mu + L, \dots) = B_\mu \Phi(\dots, x_\mu, \dots) B_\mu^\dagger. \quad (36)$$

For the particular case of one-site matrix models, we can set $\Phi(x_1, x_2, x_3, x_4) = \Phi = \text{constant}$. For the theory on the 1^4 lattice, we consider two choices for B_μ :

$$\begin{aligned} \text{pbc: } B_\mu &= 1_N, \\ \text{Twist: } B_1 &= C_{\sqrt{N}} \otimes 1_{\sqrt{N}}, & B_2 &= S_{\sqrt{N}} \otimes 1_{\sqrt{N}}, \\ B_3 &= 1_{\sqrt{N}} \otimes C_{\sqrt{N}}, & B_4 &= 1_{\sqrt{N}} \otimes S_{\sqrt{N}}, \end{aligned} \quad (37)$$

where $C_{\sqrt{N}}$ and $S_{\sqrt{N}}$ are $\sqrt{N} \times \sqrt{N}$ (noncommuting) clock and shift matrices obeying $C_{\sqrt{N}} S_{\sqrt{N}} = e^{-i(2\pi/\sqrt{N})} S_{\sqrt{N}} C_{\sqrt{N}}$. A particular representation is

¹³Of course, for QEK-like configuration, $p = 1$, and for TEK-like configurations, $p = 2$; see, for example, [37]. However, these deductions are in perturbation theory around particular backgrounds, and the determination of p is likely nonperturbative.

$$C_{\sqrt{N}} = \text{diag}(1, \omega, \omega^2, \dots, \omega^{\sqrt{N}-1}),$$

$$S_{\sqrt{N}} = \begin{pmatrix} 0 & 1 & 0 & \cdots & 0 \\ 0 & 0 & 1 & \cdots & 0 \\ \vdots & \vdots & \vdots & \ddots & \vdots \\ 0 & 0 & 0 & \cdots & 1 \\ 1 & 0 & 0 & \cdots & 0 \end{pmatrix}, \quad (38)$$

where $\omega = \exp(2\pi i/\sqrt{N})$.

The first case in (37) is the original QCD(Adj) with periodic boundary conditions and does not lift any zero or light modes associated with holonomy, or fermions. In this case, finite- N corrections turn out to be largest, of order $1/N$.

The second case in (37) is a twist of QCD(Adj). The twist lifts all possible zero or light modes from the spectrum. In this case, finite- N corrections turn out to be of order $1/N^2$.

The action of the theory with twisted boundary conditions can be turned into a theory with periodic boundary conditions and an action with an insertion of 't Hooft flux. This is our definition of “twisted” QCD(Adj) [or TQCD(Adj)]:

$$S_{0d} = -2bN \text{Re Tr} \left(\sum_{\mu < \nu} Z_{\mu\nu} V_{\mu} V_{\nu} V_{\mu}^{\dagger} V_{\nu}^{\dagger} \right) + S_F, \quad (39)$$

where $Z_{\mu\nu}$ is the twist factor. Geometrically, $Z_{\mu\nu}$ is associated with the 't Hooft flux passing through the $(\mu\nu)$ plaquette. Here we adopt “symmetric twist”

$$Z_{\mu\nu} = Z_{\nu\mu}^* = e^{2\pi i/\sqrt{N}} \quad (\mu < \nu). \quad (40)$$

As the area enclosed by fermionic “plaquette” terms is zero, the flux passing through it is zero. Thus, fermionic action is unaltered. This procedure, apart from helping QCD(Adj) algorithmically, also cures the global instability [17–19] of the TEK model. We numerically compare the behaviors of finite- N corrections for QCD(Adj) and TQCD(Adj) below.

3. Numerical results for $N_f^D = 1$

We now discuss the Monte Carlo results for QCD(Adj) and TQCD(Adj) at zero temperature. We restrict our analysis to the case with a single Dirac fermion in adjoint representation.¹⁴

In Fig. 2, the expectation value for the absolute value of the Wilson loop (averaged over all directions),

$$|W| \equiv \frac{1}{4} \sum_{\mu=1}^4 |V_{\mu}|, \quad (41)$$

¹⁴We implemented the rational hybrid Monte Carlo algorithm [49] with the multimass conjugate gradient solver [50]. Numerical coefficients in the rational approximation necessary for the rational hybrid Monte Carlo simulation were obtained by using the simulation code provided at [51].

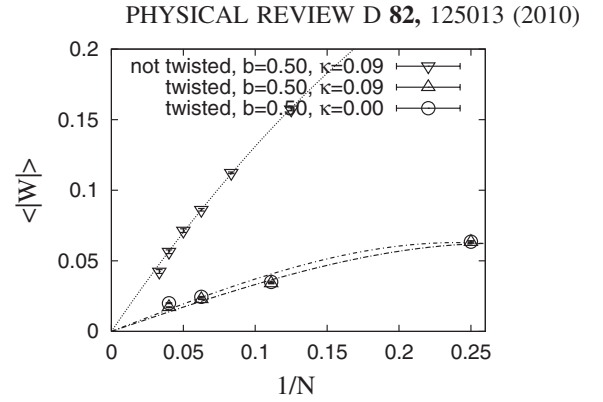


FIG. 2. Expectation values of the Wilson loop in QCD(Adj) and TQCD(Adj) at $b = 0.50$, $\kappa = 0.09$, and $\kappa = 0$ (bosonic twisted Eguchi-Kawai model). Fitting curves are of the form $c/N + d/N^2$ for the former and $c'/N + d'/N^3$ for the latter. TQCD(Adj) at $b = 0.50$, $\kappa = 0.09$, and $\kappa = 0$ agree quite well, as expected because $\kappa = 0.09$ corresponds to a quite heavy fermion.

in the QCD(Adj) and the TQCD(Adj) at zero temperature is plotted.¹⁵ For both the QCD(Adj) and TQCD(Adj), $\langle |W| \rangle$ is of order $1/N$ and hence the $(\mathbb{Z}_N)^4$ symmetry is unbroken. (As already shown in [32], it is unbroken in a rather large parameter region.) The extent of the next-to-leading correction is not clear from this plot; we fit it by $\langle |W| \rangle \sim c/N + d/N^2$ for QCD(Adj) and $\langle |W| \rangle \sim c'/N + d'/N^3$ for TQCD(Adj), where c, d, c', d' are constants.

In Fig. 3, expectation values of the plaquettes are plotted. From this plot, the finite- N correction for the QCD(Adj) turns out to be of order $1/N$. On the other hand, the finite- N correction for the TQCD(Adj) is of order $1/N^2$ as expected.

In Fig. 4, expectation values of Wilson lines $\langle |W| \rangle$ near the phase transition are shown. The argument in Sec. IV A 1 suggests the transition is of first order because several phases coexist. To confirm, we studied and observed hysteresis. We started simulation at $\kappa = 0.01$ (small- κ start) and $\kappa = 0.05$ (large- κ start), and gradually increased/decreased the value of κ . At each point, we collected 500–2000 samples, which is enough to evaluate the expectation values. As can be seen from the plot, there is a clear hysteresis. Thus we conclude the transition is indeed of first order.

We also studied the distribution of $\text{Tr}(V_{\mu} V_{\nu})/N$ as in [32], and did not find partial breaking of the center symmetry. However, around $\kappa = 0.04$ in Fig. 4, there is

¹⁵We use the absolute value of the Wilson line operator in small volume to distinguish a center-symmetric saddle point from multisaddle configurations for which $\langle W \rangle$ is nonvanishing at each saddle, but vanishes due to phase averaging over all saddles (which is permitted in quantum theory due to tunneling). Multisaddle configurations, in the large- N limit, lead to spontaneously breaking of the center symmetry, whereas a center-symmetric saddle continues to respect the center symmetry.

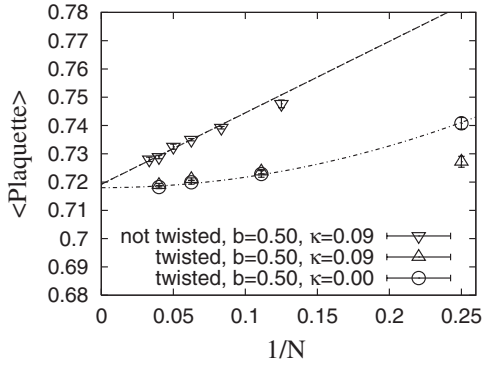


FIG. 3. Expectation values of the plaquette in QCD(Adj) at $b = 0.50$, $\kappa = 0.09$ and TQCD(Adj) at $b = 0.50$, $\kappa = 0$. The $1/N$ correction is of order $1/N$ for the QCD(Adj) and $1/N^2$ for TQCD(Adj).

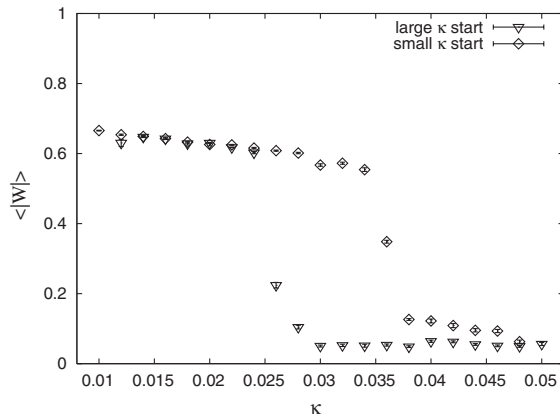


FIG. 4. Expectation values of the Wilson loop $\langle |W| \rangle$ in QCD(Adj) at $b = 0.50$, $N = 25$. Clear hysteresis can be seen.

some discrepancy between $\langle |W| \rangle$ in the large- κ start and that in the small- κ start. Hysteresis continues with a smaller gap within $0.0375 < \kappa < 0.0475$. This may be interpreted as a partial breakdown of center symmetry [52], where the unbroken phase coexists with a partially broken phase.

B. One-dimensional lattice: Reduced model at finite temperature

We first introduce a one-dimensional lattice formulation corresponding to the large- N reduced model at finite temperature and then apply two different types of twists to this model. An implication of volume independence is that one can study confinement/deconfinement transition on $\mathbb{R}^3 \times S^1_\beta$ on the equivalent unitary matrix model, corresponding to a $1^3 \times N_t$ lattice so long as $(\mathbb{Z}_N)^3$ center symmetry associated with the spatial cycles is not spontaneously broken. We indeed observe the confinement/deconfinement transition in the reduced model. For the comparison of $1/N$ corrections, we also plot some numerical results for the QCD(Adj) (without twist) at finite temperature.

1. (T)QCD(Adj) at finite temperature

On the $1^3 \times N_t$ lattice or $T^3 \times S^1_\beta$ continuum formulations, the relation between twisted boundary conditions, zero (or light) modes, and suppression of finite- N effects can systematically be studied.

Let $\Phi(t, x, y, z)$ denote either a unitary gauge field or an adjoint fermion field. We impose, the following generalized boundary conditions on fields:

$$\begin{aligned}\Phi(t, x + L, y, z) &= A\Phi(t, x, y, z)A^\dagger, \\ \Phi(t, x, y + L, z) &= B\Phi(t, x, y, z)B^\dagger, \\ \Phi(t, x, y, z + L) &= \Phi(t, x, y, z).\end{aligned}\quad (42)$$

For the particular case of matrix models, we can set $\Phi(t, x, y, z) = \Phi(t)$. We consider three choices for A and B :

$$\begin{aligned}\text{pbc} : A &= 1_N, \quad B = 1_N, \\ \text{Twist 1} : A &= C_{\sqrt{N}} \otimes 1_{\sqrt{N}}, \quad B = S_{\sqrt{N}} \otimes 1_{\sqrt{N}}, \\ \text{Twist 2} : A &= C_N, \quad B = S_N,\end{aligned}\quad (43)$$

where C_N and S_N are $N \times N$ clock and shift matrices defined earlier.

The first case in (43) is the original QCD(Adj) with periodic boundary conditions and does not lift any zero or light modes associated with holonomy, or fermions. In this case, finite- N corrections turn out to be of order $1/N$.

The second case in (43) is a partial twist of QCD(Adj). The twist lifts a $1/\sqrt{N}$ fraction of bosonic light modes and fermionic zero modes (in cases where fermions are light). This can be seen by explicitly solving the boundary conditions. In this case, finite- N corrections turn out to be of order $1/N^{3/2}$. This is explained below after introducing the twisted model.

The third case in (43) is a twist of QCD(Adj), which lifts all bosonic light modes and fermionic zero modes. This can be seen by explicitly solving the boundary conditions. In this case, finite- N corrections seem to be rather tame.

We study the theory reduced to a one-dimensional $SU(N)$ unitary matrix model

$$\begin{aligned}S_{\text{lat}} &= -2bN \sum_t \text{Re Tr} \left(\sum_i U_i(t) V_i(t+1) U_i^\dagger(t) V_i^\dagger(t) \right. \\ &\quad \left. + \sum_{i < j} Z_{ij} V_i(t) V_j(t) V_i^\dagger(t) V_j^\dagger(t) \right) + S_F,\end{aligned}\quad (44)$$

where $V_i(t)$ ($i = 1, 2, 3$) corresponds to the link variable along the spatial direction in the four-dimensional theory. For the usual nontwisted model $Z_{ij} = 1$ and $Z_{ii} = 0$, while, for twisted models, Z_{ij} is given by¹⁶

¹⁶In simulations, we use a symmetric twist which is more efficient. The above boundary conditions can be modified to incorporate the symmetric twists.

$$\begin{aligned} \text{Twist 1: } Z_{ij} &= Z_{ji}^* = e^{2\pi i/\sqrt{N}} \quad (i < j), \\ \text{Twist 2: } Z_{ij} &= Z_{ji}^* = e^{2\pi i/N} \quad (i < j). \end{aligned} \quad (45)$$

The number of sites N_t is related to the temperature T by $\beta = 1/T = aN_t$. The fermionic part S_F is given by

$$S_F = \sum_{f=1}^{N_f^D} \bar{\psi}_f D_W^{(f)} \psi_f, \quad (46)$$

where D_W is the usual Wilson-Dirac operator. The explicit form of S_F after reducing the spatial directions is

$$\begin{aligned} S_F = \sum_t & \left(\bar{\psi}(t) \psi(t) - \kappa \sum_{i=1}^3 \{ \bar{\psi}(t) (1 - \gamma_i) V_i(t) \psi(t) V_i^\dagger(t) \right. \\ & + \bar{\psi}(t) (1 + \gamma_i) V_i^\dagger(t) \psi(t) V_i(t) \} - \kappa \{ \bar{\psi}(t) (1 - \gamma_t) \\ & \times U_t(t) \psi(t+1) U_t^\dagger(t) + \bar{\psi}(t) (1 + \gamma_t) U_t^\dagger(t-1) \\ & \left. \times \psi(t-1) U_t(t-1) \} \right). \end{aligned} \quad (47)$$

We impose antiperiodic boundary condition for the fermions on the S_β^1 and generalized boundary conditions given in (43) on reduced directions. The action has a global center symmetry, which we split for convenience as $(\mathbb{Z}_N)^3 \times \mathbb{Z}_N$,

$$\begin{aligned} V_i(t) &\rightarrow e^{2\pi i/N} V_i(t), \\ (U_{t=1} \dots U_{t=N_t}) &\rightarrow e^{2\pi i/N} (U_{t=1} \dots U_{t=N_t}). \end{aligned} \quad (48)$$

If the $(\mathbb{Z}_N)^3$ symmetry is not spontaneously broken, then this model is equivalent to the one in the infinite spatial volume lattice. This implies the phase transition of infinite volume theory, associated with the realization of the temporal \mathbb{Z}_N factor, can be studied by using the unitary matrix model.

The relation between the twists, number of light modes, and the observed form of the finite- N corrections is

Twist	Zero modes	Finite- N corr.
None	N	$1/N$
$e^{i(2\pi/\sqrt{N})}$	\sqrt{N}	$1/N^{3/2}$
$e^{i(2\pi/N)}$	None	$1/N^2$

There is a nice geometric interpretation for twist 1 in terms of a classical background, and foliation of the non-commutative plane. This gives, in perturbation theory, that effective volume should scale as $V \sim N^{3/2}$. However, for twist 2, there is no classical background solution. Because of strong quantum fluctuations, a classical background cannot be written. Of course, this is not a concern.

The emergence of $V \sim N^{3/2}$ in the case of twist 1 can be explained in perturbation theory as follows: For simplicity, let us again consider the twist $Z_{12} = e^{2\pi i/\sqrt{N}}$, $Z_{13} = Z_{23} = 1$. A natural candidate of the ground state is

$$\begin{aligned} V_1 &= C_{\sqrt{N}} \otimes \mathbf{1}_{\sqrt{N}}, \\ V_2 &= S_{\sqrt{N}} \otimes \mathbf{1}_{\sqrt{N}}, \\ V_3 &= \mathbf{1}_{\sqrt{N}} \otimes C_{\sqrt{N}}. \end{aligned} \quad (49)$$

This is because this configuration satisfies $V_i V_j = Z_{ij}^* V_j V_i$, and at the same time eigenvalues spread as uniformly as possible. This configuration keeps the $(\mathbb{Z}_{\sqrt{N}})^3$ subgroup of the center symmetry, which is enough for the Eguchi-Kawai reduction to work. Then, along V_1 and V_2 directions \sqrt{N} sites arise as a fuzzy torus, similar to TEK, and \sqrt{N} sites emerges along the V_3 direction similar to QEK. So this configuration corresponds to $V^{\text{eff}} \sim N^{3/2}$ lattice sites. If one views finite- N corrections around $N = \infty$ analogous of finite-volume corrections in compactified theories, then it is expected that finite- N corrections in the one-dimensional reduced model should be a power series expansion in $1/N^{3/2}$.

2. Monte Carlo simulation for $N_f^D = 1$

Here we show the Monte Carlo results for the one-dimensional lattice model for $N_f^D = 1$. The numerical algorithm adopted is the same as the one in the previous subsection.

First let us see that the $(\mathbb{Z}_N)^3$ center symmetry is not broken. In Fig. 5, we plot the expectation value of an averaged Wilson line given by

$$|W| \equiv \frac{1}{3N_t} \sum_{i=1}^3 \sum_{t=1}^{N_t} |V_i(t)|, \quad (50)$$

at $b = 0.5$ and various κ , and $N_t = 1$ for QCD(Adj). As expected, the $(\mathbb{Z}_N)^3$ is not broken when quarks are sufficiently light for both models. We can see similar behavior for the TQCD(Adj) except for the finite- N corrections. From Figs. 6 and 7, it is clearly seen that $\langle |W| \rangle$ goes to zero as $1/N$ for the QCD(Adj) while $1/N^{3/4}$ for the TQCD

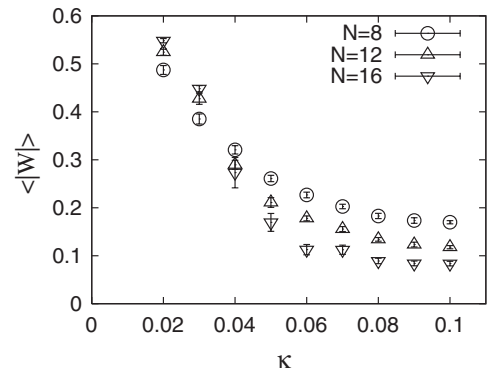


FIG. 5. Expectation value of the spatial Wilson line in QCD (Adj) (without twist) at $b = 0.50$. When the quark is lighter, the Wilson line becomes zero at large- N ; that is, $(\mathbb{Z}_N)^3$ center symmetry is not broken.

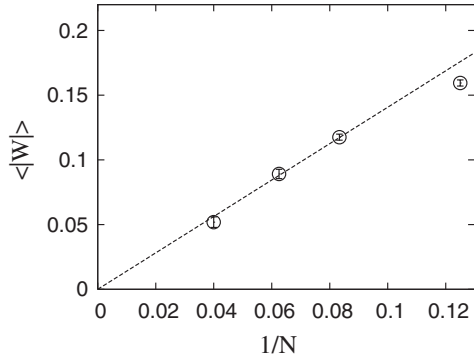


FIG. 6. $\langle |W| \rangle$ at $b = 0.50$, $\kappa = 0.10$, $N_t = 1$ for (nontwisted) QCD(Adj).

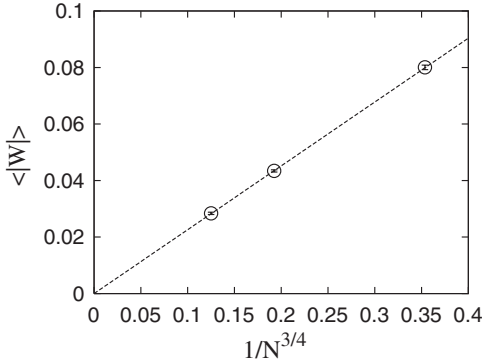


FIG. 7. $\langle |W| \rangle$ at $b = 0.50$, $\kappa = 0.10$, $N_t = 1$ for TQCD(Adj).

(Adj). That the Wilson line behaves as $\langle |W| \rangle \sim N^{-3/4} = 1/\sqrt{V}$ for the TQCD(Adj) is the same as what happened in the model in the previous section. The same pattern can also be observed with $N_t > 1$.

In Fig. 8, the plaquette is plotted for the QCD(Adj) and TQCD(Adj) with two types of twist. The Ansatz $\text{const.} + \text{const.}/N^{3/2}$ for the twist 1 is consistent with the data, and by assuming it, the extrapolated value at $N = \infty$ agrees

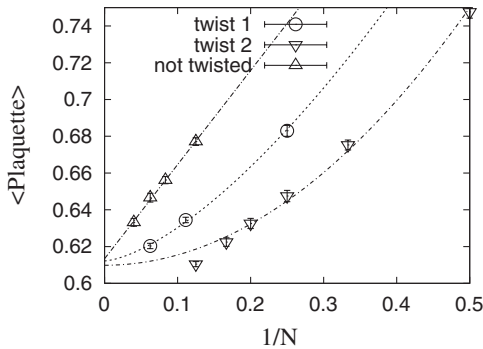


FIG. 8. Expectation value of the plaquette along spatial directions, $b = 0.50$, $\kappa = 0.10$, $N_t = 1$. Fitting Ansätze are $a + b/N$ and $a + b/N^{3/2}$ and $a + b/N^2$ for nontwisted, twist 1, and twist 2 models, respectively. For twist 2, the $N = 8$ point is not used for fitting.

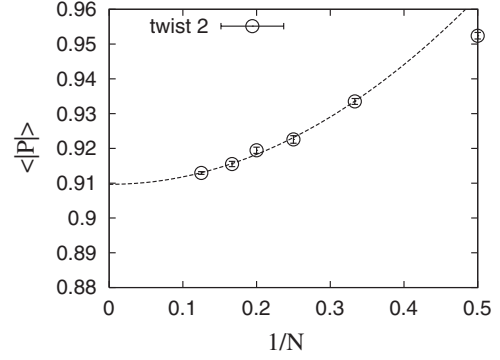


FIG. 9. Expectation value of the Polyakov loop, $b = 0.50$, $\kappa = 0.10$, $N_t = 1$. Fitting Ansatz is $a + b/N^2$.

with the one obtained from the nontwisted model. For twist 2, $\text{const.} + \text{const.}/N^2$ is consistent with the data. In Fig. 9, a similar behavior can be seen for the expectation value of the Polyakov loop defined by (51):

$$|P| = \frac{1}{N} \left| \text{Tr} \prod_{t=1}^{N_t} U_t(t) \right|, \quad (51)$$

We observe that by using twist 2, we can suppress finite- N corrections more. We notice that, up to $N = 25$, we do not observe the jump in the expectation value of the plaquette, which corresponds to the bulk transition.

Now, let us consider the confinement/deconfinement phase transition in the large- N reduced model at finite temperature. We take $\kappa = 0.10$. From the experience in pure bosonic Yang-Mills theory, which is studied extensively in [40,41], it is known that one has to take the number of spatial links N_s to be large (roughly $N_s \gtrsim 2N_t$) in order to see the deconfinement transition clearly. For QCD(Adj) without twist this is a rather severe constraint, because N_s^{eff} is related to the number of colors N by $N_s^{\text{eff}} \sim N^{1/3}$. As a result, at $N_t = 2$, we could not observe the transition below $N = 30$, although we could observe a clear transition for $N_t = 1$. In contrast, in TQCD(Adj), the transition can be seen at small values of N . In Fig. 10 we

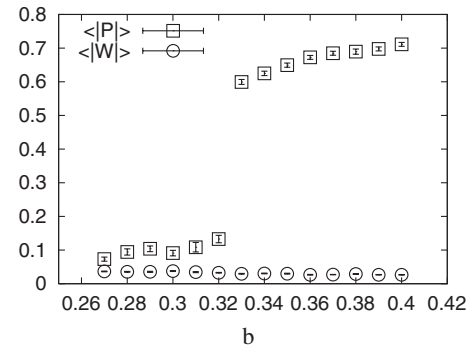


FIG. 10. Expectation values of the Polyakov loop and Wilson line at $N = 16$, $N_t = 2$, $\kappa = 0.10$.

plot the expectation value of the Wilson line and the Polyakov loop for $N_t = 2$. We can clearly see a jump of the expectation values of the Polyakov loop around $b = 0.33$ for $N_t = 2$, which corresponds to the confinement/deconfinement transition.¹⁷ This result is consistent with the one given by large volume simulations for pure Yang-Mills theory [for example, $SU(8)$ YM theory simulated on the $10^3 \times 5$ lattice gives, in the extrapolated infinite volume limit, $b_c \sim 0.34$ [40,41]], confirming the finite-temperature version of equivalence nonperturbatively.

Before closing this section, let us give an estimate for the physical temperature of the transition. By using the 2-loop beta function of the bosonic Yang-Mills theory (neglecting fermions because they are heavy), b is related to be the temperature T and lattice lambda parameter Λ_{LAT} as

$$\frac{T}{\Lambda_{\text{LAT}}} = \frac{1}{N_t} \left(\frac{11}{24\pi^2} \lambda \right)^{51/121} \exp\left(\frac{12\pi^2}{11\lambda}\right), \quad (52)$$

where $\lambda = 1/(2b)$. If we take Λ_{LAT} to be of order $\mathcal{O}(1 \text{ MeV})$ as in the QCD with $SU(3)$, by substituting it to (52), the transition temperature turns out to be of order $\mathcal{O}(100 \text{ MeV})$, as expected.

V. STABILIZING NONCOMMUTATIVE YANG-MILLS THEORY

There is a well-know perturbative equivalence between the TEK model and noncommutative YM theory. Nonperturbatively, this relation is problematic due to a global instability [17–20]. In the perturbative description, the twist-eater background is used to generate a fuzzy torus, the noncommutative base space of target theory. The spontaneous center-symmetry breaking in the TEK model is associated with the spontaneous collapse of the noncommutative torus. This instability, in effect, is related to the center-symmetry breaking instability of the TEK model. For a nice discussion of the relation between noncommutative theories and matrix models, see [53].

In this work, we suggest that TQCD(Adj) can be used to define Yang-Mills theory on noncommutative space (for recent developments, see, e.g., [54]).

As asserted above, TEK construction is problematic due to instability of the twist-eater background [17–20]. Similar construction with the fuzzy sphere also fails [20]. In noncommutative field theory, this instability corresponds to tachyonic modes in gluon propagator [55,56].

When adjoint fermions are introduced, the situation is different. The center symmetry is stabilized even at the one-site lattice and the twist-eater configuration is stable. Hence TQCD(Adj) with appropriate parameter

scalings can serve as a nonperturbative formulation of noncommutative Yang-Mills theory with adjoint fermions. The interesting point is that the background is stable even if fermions are very heavy. In such a situation, low energy physics is almost a bosonic one, but instability in the one-site model is removed thanks to fermion induced stabilizing effects. We expect that the same effect can also be achieved by introducing a twist to the double-trace deformation of the Eguchi-Kawai model [31], which is purely bosonic.

VI. CONCLUSIONS AND DISCUSSIONS

In this paper, we investigated the volume reduction for large- N gauge theory with adjoint fermions [7]. We used perturbative one-loop analysis crucially supplemented with the estimates of nonperturbative quantum fluctuations to analytically explain the zero temperature result of Ref. [32]. We have shown that for heavy fermions there exists a large-small volume equivalence, with an intermediate volume dependent phase. In the sense of dynamics, the theory exhibits a $4d-0d-4d$ cascade of dimensions. We have used the small volume phase to extract results for large volume theory.

Next, we generalized the volume independence to finite temperature, and confirmed it numerically. In effect, we have constructed a one-dimensional lattice model and analyzed it by using Monte Carlo simulation to directly show that the center symmetry is preserved for a wide parameter region including heavy fermions. In particular, we introduced a twisted version of the large- N reduced theory with adjoint fermions for numerical efficiency and then succeeded in observing the confinement/deconfinement transition. The temperature agrees with large volume simulations of pure Yang-Mills theory. We also argued that TQCD(Adj) with appropriate parameter scaling can serve as a nonperturbative formulation of noncommutative Yang-Mills theory.

There are several directions for future research. Our discussion of QCD(Adj) with the $N_f^D = 1$ fermion can be generalized to address mass spectrum and other nonperturbative aspects. By introducing more fermion flavors, our reduced models may be used to address the conformality or confinement problem, to address the determination of the lower boundary of the conformal window, and perhaps to study models relevant to the technicolor scenario.

In this work, we have seen that due to nonperturbative quantum fluctuations the restoration of full center symmetry occurs not at $mLN \sim \text{few}$, but at $mL \sim \text{few}$. This suggests that the number of double-trace operators suggested in [31] for theories on T^4 and $T^3 \times \mathbb{R}$ is a conservative overestimation, and might be reduced considerably without spoiling unbroken center symmetry. If so, since deformed reduced theories are purely bosonic, the simulation cost becomes cheaper and it can be a practical tool. If it works, it can be used as a template to study QCD with fundamental matter.

¹⁷In order to take the continuum limit, we need to analyze large N_t . However, to do this, we also need to take N large such that $N_s^{\text{eff}} \geq 2N_t$. It is beyond our current numerical resources and we leave detailed analysis for larger N_t for future work.

ACKNOWLEDGMENTS

The authors would like to thank Adi Armoni, Barak Bringoltz, Masafumi Fukuma, Antonio Gonzalez-Arroyo, Hikaru Kawai, Erich Poppitz, Steve Sharpe, and Larry Yaffe for stimulating discussions and comments. Very special thanks to Barak Bringoltz for providing his numerical data, which was very useful for checking consistency of our simulation code. The authors would also like to thank organizers and participants of “MCFP Workshop on Large- N Gauge Theories” for hospitality and useful conversations. T. A. would like to thank Weizmann Institute of Science and Albert Einstein Institute for hospitality, where a part of this work was done; he is supported by the Japan Society for the Promotion of Science (JSPS) and by the grant-in-aid for the Global COE program “The Next Generation of Physics, Spun from Universality and Emergence” from the MEXT. M. Ü. expresses his gratitude to Weizmann Institute of Science for hospitality; his work was supported by the U.S. Department of Energy Grant No. DE-AC02-76SF00515. M. H. and M. Ü. thank Aspen Center for Physics where portions of this work was done. The numerical computations in this work were in part carried out on clusters at the Yukawa Institute.

APPENDIX: QCD(ADJ) ON CONTINUUM T^4 AT FINITE- L AND ONE-LOOP ANALYSIS

In this appendix, we will rewrite the one-loop potential on small- T^4 (14) in terms of Wilson lines by using Poisson resummation. Poisson resummation is a duality which maps a sum over KK-momenta given in (14) to a sum over a winding number. The two are equivalent expressions, and some aspect of physics is more transparent in one of the two.

Since (14) is periodic under $\theta_\mu^{ab} \rightarrow \theta_\mu^{ab} + 2\pi$, it can be Fourier expanded:

$$S_{1\text{-loop}}[\theta_\mu^{ab}] = \sum_{a < b} \sum_{\vec{n} \in \mathbb{Z}^4 \setminus \{0\}} e^{i\vec{\theta}^{ab} \cdot \vec{n}} P_{\vec{n}}(mL). \quad (\text{A1})$$

For a given winding number $\vec{n} \equiv (n_1, \dots, n_4)$,

$$\begin{aligned} \sum_{a < b} e^{i\vec{\theta}^{ab} \cdot \vec{n}} &= \frac{1}{2} \sum_{a,b} e^{i\vec{\theta}^{ab} \cdot \vec{n}} - \frac{1}{2} \sum_a 1 \\ &= \frac{1}{2} (|\text{tr}(V_1^{n_1} \cdots V_4^{n_4})|^2 - N). \end{aligned} \quad (\text{A2})$$

It is also useful to express this sum in terms of trace over adjoint representation matrices, given by

$$\Omega_{\text{adj}}(\vec{n}) = (V_1^{n_1} \cdots V_4^{n_4}) \otimes (V_1^{n_1} \cdots V_4^{n_4})^\dagger, \quad (\text{A3})$$

or, equivalently,

$$\Omega_{\text{adj}}(\vec{n}) = \begin{bmatrix} \mathbf{1}_{N \times N} & & & \\ & e^{i(\vec{\theta}_1 - \vec{\theta}_2) \cdot \vec{n}} & & \\ & & \ddots & \\ & & & e^{i(\vec{\theta}_a - \vec{\theta}_b) \cdot \vec{n}} & \\ & & & & \ddots \end{bmatrix}. \quad (\text{A4})$$

Clearly, $\text{tr} \Omega_{\text{adj}}(\vec{n}) = |\text{tr}(V_1^{n_1} \cdots V_4^{n_4})|^2$. Equation (14) can dually be rewritten as a sum over winding modes

$$\begin{aligned} S_{1\text{-loop}}[V_1, \dots, V_4] &= \frac{2}{\pi^2} \sum_{a < b} \sum_{\vec{n} \in \mathbb{Z}^4 \setminus \{0\}} \frac{1}{|\vec{n}|^4} (-1 + N_f^D m^2 L^2 |\vec{n}|^2 \\ &\quad \times K_2(mL|\vec{n}|)) \cdot \cos(\vec{n} \cdot \vec{\theta}^{ab}) \\ &\equiv \frac{1}{\pi^2} \sum_{\vec{n} \in \mathbb{Z}^4 \setminus \{0\}} m_{\vec{n}}^2 (|\text{tr}(V_1^{n_1} \cdots V_4^{n_4})|^2 - N), \end{aligned} \quad (\text{A5})$$

where $m_{\vec{n}}^2$ is interpreted as the mass square of the Wilson line with winding number \vec{n} . Unlike the similar sums appearing in one-loop effective potential on $\mathbb{R}^{4-d} \times T^d$ with $1 \leq d \leq 3$ which are absolutely convergent [7], the series (A5) is conditionally convergent.¹⁸ This is, of course, physical and related to nontrivial infrared (IR) aspects of the theory which we discuss below.

IR singularities, conditional convergence, and noncommutative saddles

The series in (14) and (A5) are equivalent expressions, related to each other via Poisson resummation. Consider the zero KK-momenta subsector of (14). Since eigenvalue separation has an interpretation as momentum, (14) exhibits an IR singularity whenever $\sum_{\mu=1}^4 (\theta_\mu^{ab})^2 = 0$ for some a, b . This IR problem is also manifest in lattice one-site one-loop action (31). The series (A5) is conditionally convergent, and whenever two eigenvalues are coincident, $\sum_{\vec{n} \in \mathbb{Z}^4 \setminus \{0\}}$ exhibits logarithmic IR divergences due to modes with large-winding number $|\vec{n}| \rightarrow \infty$. Winding modes have an interpretation in terms of spacetime distance [25] and this is the same IR problem as in (14). The physical interpretation of divergence is as follows: Whenever two (or more) eigenvalues are coincident, there are (in perturbation theory) massless modes (analog of W bosons or open strings). IR divergence comes about because we have integrated out these massless modes that we should have kept in the correct description of long-distance dynamics of the effective theory.

¹⁸In (A5), the subtraction of the constant divergent term is related to the absence of log divergent and holonomy-independent $\sum_{a=b}$ terms in the first line, as well as (14). With this subtraction, any singularity that may appear in the sum (A5) or its dual (14) is physical IR singularity. IR aspects of one-loop effective action can be examined in either picture.

Whenever two (or more) $\sum_{\mu=1}^4 (\theta_{\mu}^{ab})^2 = 0$, the zeroth order assumption that one can expand the fluctuations around commuting saddles (4) is incorrect. There are circumstances where commutative saddle points of the classical theory may be a good description at one-loop order in perturbation theory for some range of m . For example, if $m = 0$, then the one-loop effective action (14) and (A5) reduces to

$$\begin{aligned} S_{1\text{-loop}}[\theta_{\mu}^{ab}] &= (2 - 4N_f^D) \sum_{a < b} \sum_{k_1, \dots, k_4} \log \left(\sum_{\mu=1}^4 \frac{(2\pi k_{\mu} + \theta_{\mu}^{ab})^2}{L^2} \right) \\ &= (-1 + 2N_f^D) \frac{1}{\pi^2} \sum_{\vec{n} \in \mathbb{Z}^4 \setminus \{0\}} \frac{1}{|\vec{n}|^4} (\text{tr} \Omega_{\text{adj}}(\vec{n}) - N). \end{aligned} \quad (\text{A6})$$

This one-loop action is bounded from below and generates a repulsion between eigenvalues.

If m is sufficiently large, then the one-loop action (14) and (A5) is unbounded from below and leads to an attraction between eigenvalues. A configuration where all eigenvalues clump and center is broken is the minimum. However, the action is IR divergent there. This is an artifact of perturbation theory. Whenever eigenvalues are close to each other, then the relevant scale in the theory is $\lambda_{0d}^{1/4}$, and the dynamics is strongly coupled for eigenvalues in the $|\vec{x}_{ab}| \lesssim \lambda_{0d}^{1/4}$ domain where one should not use perturbation theory.

At one-loop order in perturbation theory, the actions (14) and (A5) as well as the one-site version (31) realize all the saddles conjectured to exist in Ref. [43]. At $m = 0$, the leading fluctuations are quadratic or Gaussian; at $m = \infty$, the leading fluctuations are quartic according to the classification of Ref. [43]. As mL is dialed, all interesting saddles with a varying number of quadratic and quartic fluctuations appear in massive QCD(Adj). In Refs. [13,43], only the two extreme cases were shown to exist in pure Yang-Mills theory in d dimensions, as d is varied.

Since the one-loop action has IR singularities, the way to obtain the set of saddle points requires some care.

- (1) Introduce an auxiliary IR cutoff $\mu_{\text{IR}} \ll m$, modifying gauge contribution in (14) to $\sum_{\mu=1}^4 (2\pi k_{\mu} + \theta_{\mu}^{ab})^2 L^{-2} + \mu_{\text{IR}}^2$ [36]. At any finite but infinitesimal value of μ_{IR} , we can sensibly compare the one-loop effective action of different saddles, and find the global minima at a given value of mL . At $m = \infty$, the global minima are at $V_{\mu} = 1$ (and its center conjugates). This can be studied by using the Hermitian matrix model (15).

 bunched phase ($k=6^4$)

uniform phase

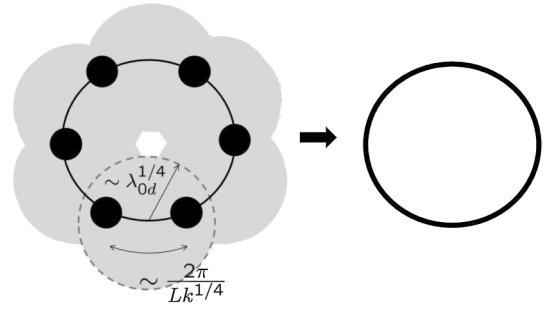


FIG. 11. If k is large enough so that the distance between two nearest bunches $2\pi/(Lk^{1/4})$ becomes smaller than the quantum fluctuation scale $\lambda_{0d}^{1/4}$, interaction between these two bunches cannot be evaluated by using one-loop effective action. Quantum fluctuation turns the k -bunch phase into the uniform phase.

- (2) Assume that the global minimum is a k -bunch configuration of Wilson line phases. The nonperturbative width of each clump, due to quantum fluctuations, is determined by the zero-dimensional matrix model. Interactions between different clumps are well approximated by one-loop effective action, and are repulsive. Dynamics inside each clump is approximated by the $SU(N/k)$ matrix model,

$$\begin{aligned} S_{\text{clump}} &= \frac{(N/k)}{(\lambda_{0d}/k)} \text{Tr} \left(-\frac{1}{4} [X'^{\mu}, X'^{\nu}]^2 \right. \\ &\quad \left. + \sum_{f=1}^{N_f^D} \bar{\psi}'_f (\gamma_{\mu} [X'^{\mu}, \psi'_f] + m \psi'_f) \right), \end{aligned} \quad (\text{A7})$$

where we put primes in order to emphasize that matrices are $(N/k) \times (N/k)$. Then, 'tHooft coupling effectively becomes λ_{0d}/k , and hence the nonperturbative width of each clump is $\sim (\lambda_{0d}/k)^{1/4}$.

- (3) At relatively large values of fermion mass, $mL \sim 1$, one may expect that only a small subgroup of $(\mathbb{Z}_N)^4$ symmetry persists. However, if k is sufficiently large that distance between bunches becomes smaller than the fluctuation scale, $2\pi/(Lk^{1/4}) \lesssim \lambda_{0d}^{1/4} = \lambda_{4d}^{1/4}/L$, interaction between nearby bunches cannot be evaluated by one-loop approximation, and distinction of bunches becomes obscure. This implies that the k -bunch phase is indistinguishable from the uniform phase. (See Fig. 11.)

- [1] A. Armoni, M. Shifman, and G. Veneziano, *Nucl. Phys.* **B667**, 170 (2003); *Phys. Rev. Lett.* **91**, 191601 (2003).
- [2] P. Kovtun, M. Ünsal, and L. G. Yaffe, *J. High Energy Phys.* **07** (2005) 008; M. Ünsal and L. G. Yaffe, *Phys. Rev. D* **74**, 105019 (2006).
- [3] E. Corrigan and P. Ramond, *Phys. Lett.* **87B**, 73 (1979).
- [4] A. Armoni and A. Patella, *J. High Energy Phys.* **07** (2009) 073.
- [5] A. Cherman, T. D. Cohen, and R. F. Lebed, *Phys. Rev. D* **80**, 036002 (2009).
- [6] C. Hoyos and A. Karch, *Phys. Rev. D* **79**, 125021 (2009).
- [7] P. Kovtun, M. Ünsal, and L. G. Yaffe, *J. High Energy Phys.* **06** (2007) 019.
- [8] T. Eguchi and H. Kawai, *Phys. Rev. Lett.* **48**, 1063 (1982).
- [9] M. Ünsal, *Phys. Rev. Lett.* **100**, 032005 (2008).
- [10] M. Ünsal, *Phys. Rev. D* **80**, 065001 (2009).
- [11] L. G. Yaffe, *Rev. Mod. Phys.* **54**, 407 (1982).
- [12] R. Narayanan and H. Neuberger, *Phys. Rev. Lett.* **91**, 081601 (2003).
- [13] G. Bhanot, U. M. Heller, and H. Neuberger, *Phys. Lett.* **113B**, 47 (1982).
- [14] G. Parisi, *Phys. Lett.* **112B**, 463 (1982); D. J. Gross and Y. Kitazawa, *Nucl. Phys.* **B206**, 440 (1982).
- [15] A. Gonzalez-Arroyo and M. Okawa, *Phys. Rev. D* **27**, 2397 (1983).
- [16] B. Bringoltz and S. R. Sharpe, *Phys. Rev. D* **78**, 034507 (2008).
- [17] W. Bietenholz, J. Nishimura, Y. Susaki, and J. Volkholz, *J. High Energy Phys.* **10** (2006) 042.
- [18] M. Teper and H. Vairinhos, *Phys. Lett. B* **652**, 359 (2007).
- [19] T. Azeyanagi, M. Hanada, T. Hirata, and T. Ishikawa, *J. High Energy Phys.* **01** (2008) 025.
- [20] T. Azeyanagi, M. Hanada, and T. Hirata, *Phys. Rev. D* **78**, 105017 (2008).
- [21] T. Ishii, G. Ishiki, S. Shimasaki, and A. Tsuchiya, *Phys. Rev. D* **78**, 106001 (2008).
- [22] E. Poppitz and M. Ünsal, *Phys. Rev. D* **82**, 066002 (2010).
- [23] A. Gonzalez-Arroyo and M. Okawa, *J. High Energy Phys.* **07** (2010) 043.
- [24] P. F. Bedaque, M. I. Buchoff, A. Cherman, and R. P. Springer, *J. High Energy Phys.* **10** (2009) 070.
- [25] B. Bringoltz, *J. High Energy Phys.* **01** (2010) 069; **06** (2009) 091.
- [26] E. Poppitz and M. Ünsal, *J. High Energy Phys.* **01** (2010) 098.
- [27] J. C. Myers and M. C. Ogilvie, *J. High Energy Phys.* **07** (2009) 095.
- [28] G. Cossu and M. D'Elia, *J. High Energy Phys.* **07** (2009) 048.
- [29] T. J. Hollowood and J. C. Myers, *J. High Energy Phys.* **11** (2009) 008.
- [30] M. Ünsal, *Phys. Rev. D* **76**, 025015 (2007).
- [31] M. Ünsal and L. G. Yaffe, *Phys. Rev. D* **78**, 065035 (2008).
- [32] B. Bringoltz and S. R. Sharpe, *Phys. Rev. D* **80**, 065031 (2009).
- [33] A. Hietanen and R. Narayanan, *arXiv:0911.2449* [*J. High Energy Phys.* (to be published)].
- [34] T. Azeyanagi, M. Hanada, T. Hirata, and H. Shimada, *J. High Energy Phys.* **03** (2009) 121.
- [35] G. 't Hooft, *Nucl. Phys.* **B72**, 461 (1974).
- [36] B. Bringoltz and S. R. Sharpe (private communication).
- [37] S. R. Das, *Rev. Mod. Phys.* **59**, 235 (1987).
- [38] A. Coste, A. Gonzalez-Arroyo, C. P. Korthals Altes, B. Soderberg, and A. Tarancon, *Nucl. Phys.* **B287**, 569 (1987).
- [39] E. Witten, *Nucl. Phys.* **B202**, 253 (1982).
- [40] B. Lucini, M. Teper, and U. Wenger, *J. High Energy Phys.* **02** (2005) 033.
- [41] M. Panero, *Phys. Rev. Lett.* **103**, 232001 (2009).
- [42] P. Austing and J. F. Wheeler, *J. High Energy Phys.* **02** (2001) 028.
- [43] A. Coste, A. Gonzalez-Arroyo, J. Jurkiewicz, and C. P. Korthals Altes, *Nucl. Phys.* **B262**, 67 (1985).
- [44] M. Hanada, S. Matsuura, J. Nishimura, and D. Robles-Llana (to be published); M. Hanada and I. Kanamori, *Phys. Rev. D* **80**, 065014 (2009).
- [45] M. Ünsal and L. G. Yaffe (unpublished).
- [46] S. Catterall and T. Wiseman, *J. High Energy Phys.* **12** (2007) 104.
- [47] K. N. Anagnostopoulos, M. Hanada, J. Nishimura, and S. Takeuchi, *Phys. Rev. Lett.* **100**, 021601 (2008).
- [48] G. 't Hooft, *Nucl. Phys.* **B153**, 141 (1979).
- [49] A. D. Kennedy, I. Horvath, and S. Sint, *Nucl. Phys. B, Proc. Suppl.* **73**, 834 (1999).
- [50] B. Jegerlehner, *arXiv:hep-lat/9612014*.
- [51] M. A. Clark and A. D. Kennedy, <http://www.ph.ed.ac.uk/~mike/remez>, 2005.
- [52] Stephen R. Sharpe (private communication).
- [53] H. Aoki, N. Ishibashi, S. Iso, H. Kawai, Y. Kitazawa, and T. Tada, *Nucl. Phys.* **B565**, 176 (2000).
- [54] H. Steinacker, *Classical Quantum Gravity* **27**, 133 001 (2010).
- [55] M. Van Raamsdonk, *J. High Energy Phys.* **11** (2001) 006.
- [56] A. Armoni and E. Lopez, *Nucl. Phys.* **B632**, 240 (2002).